Shaping of neural activity by homeostatic plasticity

A Thesis

submitted to
Indian Institute of Science Education and Research Pune
in partial fulfillment of the requirements for the
BS-MS Dual Degree Programme

by

Richa Agarwal

Indian Institute of Science Education and Research Pune
Dr. Homi Bhabha Road,
Pashan, Pune 411008, INDIA.

May, 2023

Supervisor: Suhita Nadkarni

Certificate

This is to certify that this dissertation entitled Shaping of neural activity by homeostatic plasticitytowards the partial fulfilment of the BS-MS dual degree programme at the Indian Institute of Science Education and Research, Pune represents study/work carried out by Richa Agarwal at Indian Institute of Science Education and Research under the supervision of Suhita Nadkarni, Professor, Department of Biology , during the academic year 2022-2023.

Suhita Nadkarni

Committee:

Suhita Nadkarni

Aurnab Ghose

This thesis is dedicated to my parents.

Declaration

I hereby declare that the matter embodied in the report entitled Shaping of neural activity by homeostatic plasticity are the results of the work carried out by me at the Department of Biology, Indian Institute of Science Education and Research, Pune, under the supervision of Suhita Nadkarni and the same has not been submitted elsewhere for any other degree.

Richa Agarwal

Acknowledgments

I'd like to express my sincere thanks to Prof. Suhita Nadkarni for her invaluable guidance and constructive feedback throughout the project. Her mentorship has been instrumental in helping me grow as a researcher, and her support and encouragement have been a constant source of motivation for me.

I'd like to thank our collaborators Prof. Deepak Nair and Dr. Pallavi Netrakanti, for sharing invaluable insights from their experiments on hippocampal cultures. I also wish to thank my expert member Prof. Aurnab Ghose for his constructive feedback and encouraging words.

I'd like to extend my deepest gratitude to Dr. Nishant Singh for his immense support and help during the project. His coding expertise and practical experience were instrumental in guiding me through the initial phases of working in a computational lab. I'm deeply appreciative of all the members of Nadkarni Lab and Assisi Lab for fostering a friendly and positive environment in the lab, and being incredibly helpful and inspiring.

I'm extremely grateful to the institute for providing exceptional facilities and an environment conducive to research and well-being. I'd like to acknowledge Kishore Vaigyanik Protsahan Yojana (KVPY) for generously funding me during my BS-MS in IISER.

I'd like to express my gratitude to my dearest family members and friends for their love and support. Special thanks to my roommate, Samyuktha Ramadurai, for her unwavering support and enriching discussions throughout our journey in IISER. She has been a constant companion, from when I had little clarity about my interests to when I was developing a fascination towards neuroscience to having her put up with my obsession with the project and the lab. Her presence has been a source of great comfort and motivation for me.

Contributions

Contributor name	Contributor role
Suhita Nadkarni, Richa Agarwal	Conceptualization ideas
Suhita Nadknarni, Nishant Singh, Richa Agarwal	Methodology
Richa Agarwal, Nishant Singh, Suhita Nadkarni	Software
Richa Agarwal	Validation
Richa Agarwal, Suhita Nadkarni, Nishant Singh	Formal analysis
Richa Agarwal	Investigation
Suhita Nadkarni	Resources
Richa Agarwal	Data Curation
Richa Agarwal	Writing - original draft preparation
Suhita Nadkarni, Aurnab Ghose, Richa Agarwal	Writing - review and editing
Richa Agarwal, Suhita Nadkarni, Nishant Singh	Visualization
Suhita Nadkarni	Supervision
Suhita Nadkarni, Richa Agarwal	Project administration
Suhita Nadkarni	Funding acquisition

Abstract

The positive-feedback nature of Hebbian plasticity can cause instability in neuronal networks and drive them to a state of hyperactivity or hypoactivity. Homeostatic plasticity is a crucial counter mechanism that maintains the excitability of the nervous system by modulation of synaptic strengths and membrane conductances. The regulation of synaptic strengths often occurs through various presynaptic modifications that affect the release of neurotransmitters. To understand how synaptic transmission and synaptic plasticity are affected during presynaptic homeostasis, we developed a biophysically-detailed, spatially-explicit, and stochastic model of the CA3-CA1 presynapse to describe the most significant presynaptic homeostatic modifications, such as changes in voltage-dependent calcium channel (VDCC) expression and placement and readily releasable pool (RRP) size. We chose the hippocampal CA3-CA1 synapse for our investigations since it's a highly plastic synapse important for learning and memory. Through simulations of presynaptic activity leading to vesicular release, we examined how changes in the expression and organization of VDCCs affect the probability of neurotransmitter release. We investigated the influence of presynaptic homeostatic changes on short-term plasticity (STP), given that STP has an essential role in information transmission and optimizing energetic expenditure during synaptic transmission. Our results suggest that short-term plasticity is altered during homeostatic modifications. We explored the further impact of these modifications on information transfer and energy efficiency during vesicular release. The data suggest that homeostatic changes in VDCC expression and RRP size do not affect the transfer of information but affect the specific cost of information. We also provided an explanatory framework for enhanced miniature excitatory postsynaptic current (mEPSC) frequency observed after the suppression of activity. According to our results, an increase in the readily-releasable pool size causes a proportional increase in mEPSC frequency and only partly explains the observed increase. The large magnitude of changes in mEPSC frequency can be explained by a plausible increase in cytosolic basal calcium concentration. Overall, our study investigates how presynaptic homeostatic modifications influence synaptic strength, short-term plasticity, and the transmission of information at the synapses. The changes observed in short-term plasticity suggest that homeostatic plasticity might have a dynamic role in shaping neural activity rather than merely serving as a stabilizing mechanism.

Contents

Chapter 1

Introduction

1.1 Homeostatic Plasticity

Neural networks are in a perpetual state of flux as organisms mature and adapt to their surroundings. Neurons grow in size. Their synaptic connections change as new connections are established, others are lost, and the strengths of synapses are tuned for learning to happen. Despite all these changes, how do neural networks maintain stable activity?

Hebbian plasticity, responsible for learning and memory, strengthens synapses when the postsynaptic neuron regularly fires after the presynaptic one. In the absence of a correlation between presynaptic and postsynaptic activity, synapses are weakened. However, without a stabilizing mechanism, the correlation-based rules of Hebbian plasticity would create a positive feedback loop, leading to uncontrolled strengthening or weakening of synapse (Turrigiano and Nelson, 2000; Abbott and Nelson, 2000). A neuron with some input synapses strengthened by Hebbian plasticity would become more easily excitable by any of its presynaptic neurons. This would lead to even more strengthening of the synapses, even the ones with weak activity correlations. Theoretical studies have shown such instabilities in networks governed solely by correlation-based learning rules. All synaptic weights either saturate or become zero in the absence of any constraint on the total synaptic strength (Miller and MacKay, 1994).

Homeostatic plasticity maintains the average firing rate of the neurons. It counteracts the Hebbian positive feedback loop by maintaining the excitability of the neurons and prevents the system from becoming hyperactive or hypoactive. Maintaining an optimal level of activity is essential for the proper transmission and processing of information (Turrigiano and Nelson, 2004). Fig 1.1 illustrates how hyperexcitability or hypoexcitability in a feedforward network can disrupt the representation and propagation of a signal.

1.1.1 Synaptic Scaling and Intrinsic Plasticity

The regulation of a neuron's firing rate can be achieved through modulation of its synaptic input or ion channel properties that determine its excitability.

Synaptic scaling is a process that maintains the total synaptic input to a neuron by scaling up or down the strengths of all input synapses, following any modifications made by Hebbian

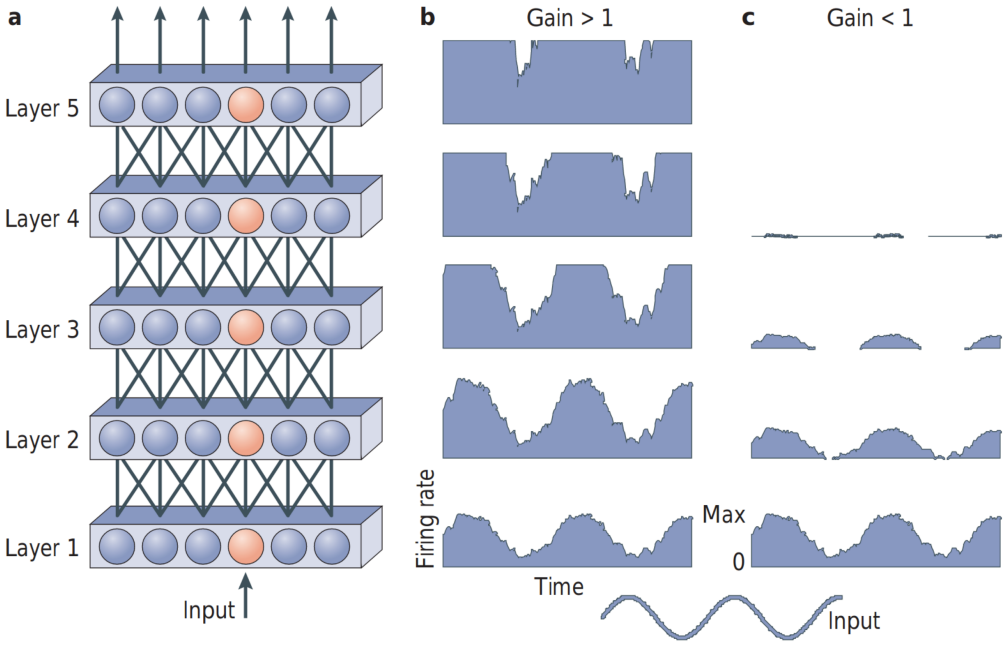

Figure 1.1: Schematic of signal propagation in a feedforward network. (a) The network with layers of neurons connected in a feedforward manner is shown. The firing rate of the red neuron in response to a sinusoidal input is shown for gain of transmission (b) greater than one, (c) when it is less than one. The signal either saturates or fails to propagate. The information about the stimulus is lost in both cases. Adapted from Turrigiano and Nelson (2004).

plasticity. The relative synaptic weights are preserved in the process, which is essential for maintaining the information encoded by Hebbian plasticity. Synaptic competition arises as a result of this process, where the strengthening of some synapses leads to the weakening of others (Abbott and Nelson, 2000; Turrigiano, 2008). Fig 1.2 illustrates the stabilisation of firing rate by scaling of AMPARs after potentiation of a synapse.

Multiplicative scaling of miniature Excitatory Postsynaptic Current (mEPSC) amplitude, an indicator of postsynaptic strength, was first observed in neocortical cultures following activity suppression by TTX, a Na+ channel blocker, as well as activity enhancement by Bicuculline, a GABA receptor antagonist. Acute bicuculline treatment significantly increased firing rates, but after 48hrs of treatment, the firing rate returned to around normal levels (Turrigiano et al., 1998).

While synaptic homeostasis regulates inputs to neurons, modulation of the voltage-dependent sodium, potassium, and calcium conductances can alter the threshold for spike

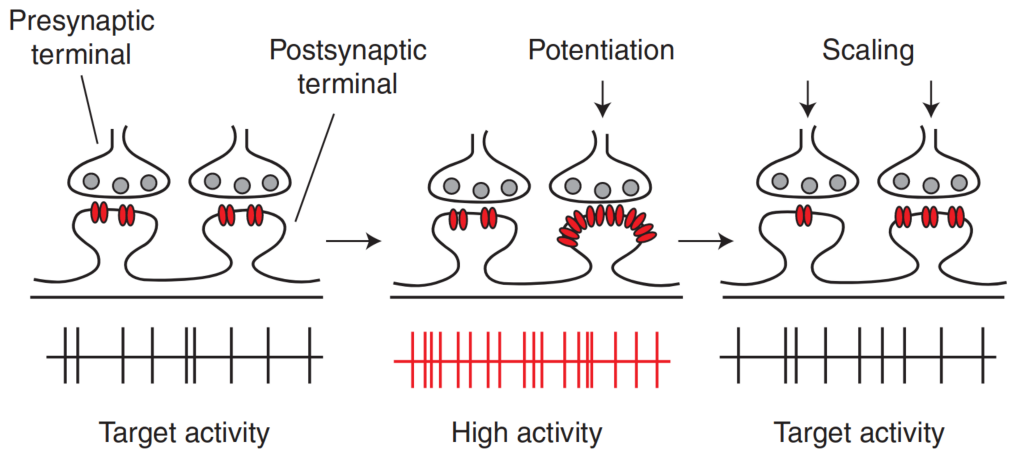

Figure 1.2: Stabilization of activity via synaptic scaling. The potentiation of a synapse causes an increase in the firing rate. Scaling down synaptic strengths through number of AMPARs brings the activity back to normal. Illustration reproduced from Turrigiano (2012).

generation, and hence regulate firing rate by affecting neuronal response to a stimulus (Turrigiano and Nelson, 2000). Fig 1.3 depicts how regulation of firing rate via intrinsic plasticity differs from that via synaptic scaling. Intrinsic plasticity shifts the response curve of the neuron so that a different firing rate can be achieved for the same input.

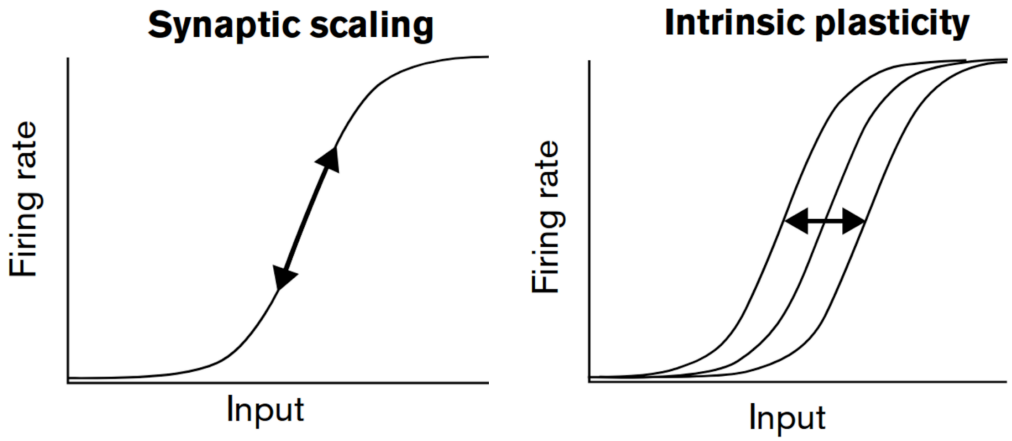

Figure 1.3: Synaptic scaling vs Intrinsic plasticity. Synaptic scaling modulates synaptic drive to the neuron. Intrinsic plasticity shifts the response curve of the neuron to regulate the firing rate without affecting the synaptic input. Adapted from Turrigiano and Nelson (2000).

1.1.2 Presynaptic and Postsynaptic Mechanisms

The strength of synapses can be modulated through modifications in the machinery responsible for releasing neurotransmitters at the presynapse, or through changes in the reception of these neurotransmitters at the postsynapse. In vitro studies frequently use alterations in miniature excitatory postsynaptic currents (mEPSCs) to identify such modifications following pharmacological manipulations of activity. mEPSCs represent the postsynaptic neuronal response to a single vesicle's spontaneous fusion at the presynapse, in the absence of external stimulation. Changes in the frequency of mEPSCs reflect modifications at the presynapse, whereas changes in amplitude indicate postsynaptic modifications.

Figure 1.4 shows the changes in mEPSC frequency and amplitude following TTX treatment of hippocampal cultures at different developmental stages (Han and Stevens, 2009). The maturity of the neurons appears to affect whether presynaptic or postsynaptic mechanisms are employed. Wierenga et al. (2006) demonstrated that the number of days spent in vitro before pharmacological treatment, rather than the age of the neurons, is a determining factor. The homeostatic response is also shown to be synapse-specific (Kim and Tsien, 2008), and the changes observed depend on how the activity is manipulated. These studies reveal the context-dependent nature of the homeostatic response. Presynaptic and postsynaptic mechanisms may work exclusively or in conjunction to bring about the required changes in activity.

The regulation of vesicle pool size and presynaptic Ca^{2+} flux are considered to be the prominent mechanisms working at the presynapse during homeostasis (Zhao et al., 2011; Jeans et al., 2017; Delvendahl and Müller, 2019). An increase in Readily Releasable Pool

	8div 24 h TTX	9 div 48 h TTX	15 div 24 h TTX	16 div 48 h TTX
mEPSC frequency	-	-	⇑	⇑
mEPSC amplitude	⇑	-	-	⇑

Figure 1.4: Table adapted from Han and Stevens (2009). The effect on mEPSC frequency and amplitude following TTX treatment depends on the duration of the treatment and the maturity of hippocampal cultures (div denotes days in vitro).

size and Ca^{2+} flux by P/Q-VDCCs was reported in hippocampal neurons in response to activity blockage by TTX (Jeans et al., 2017). Changes in the opposite direction were seen for inhibition suppression by GABA antagonists. These modifications regulate the strengths of synapses by their effect on the release probability of vesicles at the presynapse (Murthy et al., 2001; Zhao et al., 2011; Jeans et al., 2017).

1.2 Motivation and Research Interests

Several studies have observed presynaptic modifications, such as changes in the Readily Releasable Pool size and calcium influx through VDCCs, after activity manipulations in hippocampal cultures (Thiagarajan et al., 2005; Han and Stevens, 2009; Zhao et al., 2011; Jeans et al., 2017). Such changes regulate synaptic strength through their effect on synaptic release probability. Changes in release probability (Pr) during homeostasis would be accompanied by changes in short-term plasticity, as indicated by the inverse relationship between the Pr and Paired-Pulse Ratio (Manabe et al., 1993; Debanne et al., 1996; Dobrunz and Stevens, 1997) Increased calcium flux, as seen following activity suppression, can rapidly deplete vesicles, making the synapse more susceptible to short-term depression. In hippocampal slice experiments, increased susceptibility to short-term depression was observed in evoked Excitatory Postsynaptic Current (eEPSC) responses to 20Hz simulations in CA3-CA3 synapses and DG-CA3 synapses after TTX treatment (Kim and Tsien, 2008). Delvendahl et al. also reported a reduction in the paired-pulse ratio in cerebellum mossy fiber synapses after pharmacological AMPAR perturbation in a genetic model of presynaptic homeostatic plasticity (Delvendahl et al., 2019). Given its crucial role in information transmission and processing at synapses, how short-term plasticity is modified during homeostasis, considered a stabilizing mechanism, becomes an interesting question.

Reorganization of VDCCs and an increase in their density in synapses of hippocampal cultures following activity suppression via TTX has been observed recently (Netrakanti and Nair, 2021). The researchers also observe multiplicative scaling of VDCC's average fluorescence intensity in the synapses after the TTX treatment. The results provide additional insights into the presynaptic changes that happen during homeostasis. Given that synaptic scaling of strengths through a postsynaptic mechanism has been demonstrated, how multiplicative scaling of VDCCs affects synaptic strength is worth exploring, as homeostatic

presynaptic modifications must occur while ensuring the preservation of relative synaptic weights.

To address these questions, the biophysically detailed and spatially explicit model of vesicular release at CA3-CA1 synapse developed by Nadkarni and colleagues provides a powerful tool for gaining mechanistic insights into the effect of these presynaptic changes on synaptic transmission and short-term plasticity. We develop the model to describe the most significant changes that happen during presynaptic homeostasis, such as changes in VDCC expression and placement and readily releasable pool size, to understand their influence on short-term plasticity. We investigate how tradeoff between information transfer and energy use is affected as a result of short-term plasticity changes observed during homeostasis. Using our model, we also quantify the effect of changes in VDCC density, organization and multiplicative scaling on release probability to understand how synaptic weights are regulated by such modifications. Additionally, we seek to uncover potential explanations for mEPSC frequency changes that are observed following presynaptic homeostasis.

Chapter 2

Methods

2.0.1 Spatial Model of CA3-CA1 presynapse

The biophysical, spatially explicit, stochastic model of the CA3-CA1 presynapse, as described in the study by Nishant and colleagues, was used to simulate vesicle release for various synaptic configurations (Singh et al., 2021; Nadkarni et al., 2010). Simulations were performed using Monte Carlo cell (https://mcell.org/), which tracks the diffusion of each molecule and carries out the reactions defined by the user (Stiles et al., 1996, 2001; Kerr et al., 2008). We have used the canonical version of the model with simplified cuboidal geometry representing a canonical presynapse of average dimensions $4 \times 0.5 \times 0.5$ µm (Fig 2.1). The model contains an ER compartment of dimensions $3.9 \times 0.1 \times 0.1$ µm.

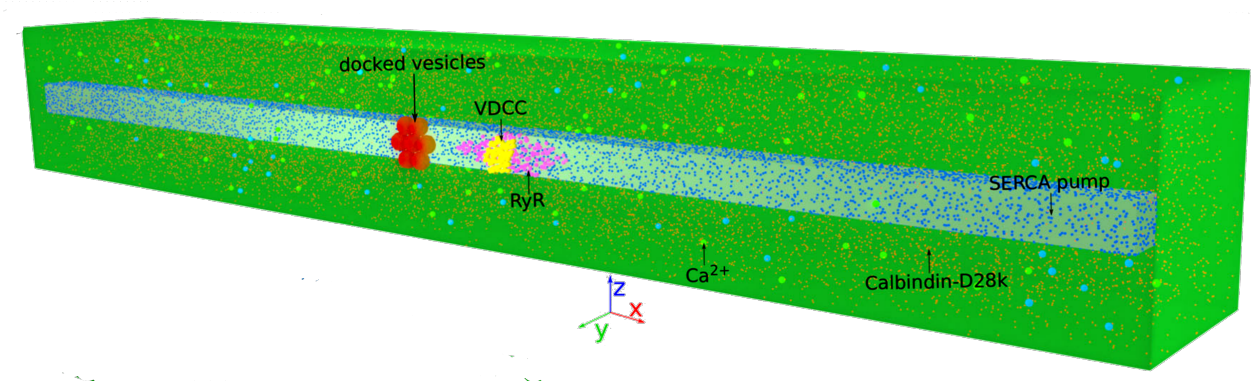

Figure 2.1: Spatial model of the presynapse with simplified geometry. The model consists of calcium channels: VDCC and RyR; calcium pumps: PMCA and SERCA; and the calcium buffer: calbindin-D28K. VDCCs and PMCA pumps are located on the plasma membrane; RyRs and SERCA pumps on the ER membrane. Vesicles are docked at the release site, and VDCCs are clustered at a distance from the release site. Adapted from Singh et al. (2021).

The model simulates the diffusion and reaction kinetics of the molecules leading to the fusion of vesicles in response to an input stimulus. Calbindin buffers the calcium as it enters through Voltage-Dependent Calcium Channels (VDCCs) in response to an action potential. Ryanodine Receptors (RyRs), located on the ER, open on binding to calcium. Because of the higher concentration of calcium in ER, calcium effluxes out on the RyR opening. SarcoEndoplasmic Reticulum Calcium ATPase (SERCA) and Plasma Membrane Calcium ATPase (PMCA) pump calcium out of the cytosol. Vesicle is fused when enough calcium ions bind to either the synchronous calcium sensor or the asynchronous calcium sensor. The two sensors differ in their binding affinity to calcium and the number of ions they bind to before leading to the fusion. The kinetic schemes for the binding of calcium to different

transporters and the calcium buffer are shown in fig. 2.2. The kinetic schemes for calcium binding to sensors for synchronous and asynchronous release is shown in fig. 2.3.

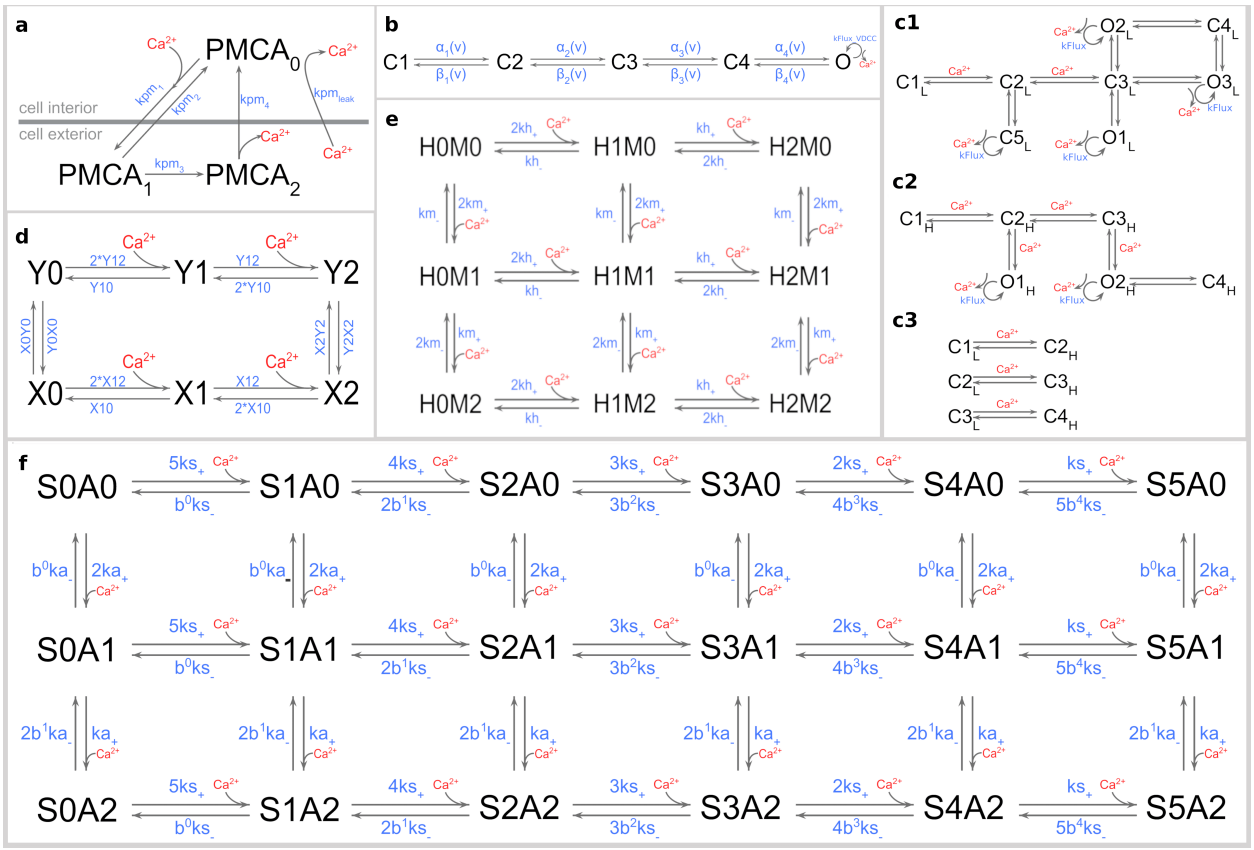

Figure 2.2: Kinetic schemes. (a) PMCA. Calcium is transported out of the cytosol via the transition from $PMCA_0$ to $PMCA_1$. The scheme also incorporates calcium leak through the plasma membrane. (b) VDCC. Channel transitions between closed and open states through voltage-dependent kinetic rates. Calcium is conducted in the "O" state. (c) RyR. (c1) Low activity states, (c2) high activity states, and (c3) transition between low and high states. "O" are the open states that allow calcium flux. (d) SERCA. The binding site "X" is on the cytosolic side, and "Y" is on the ER side. Calcium is transported into the ER via the transition from X2 to Y2. (e) Calcium buffer, Calbindin-D28k. Calbindin is modeled to have two high-affinity sites and two medium-affinity sites, each of which binds two calcium. Adapted from Singh et al. (2021).

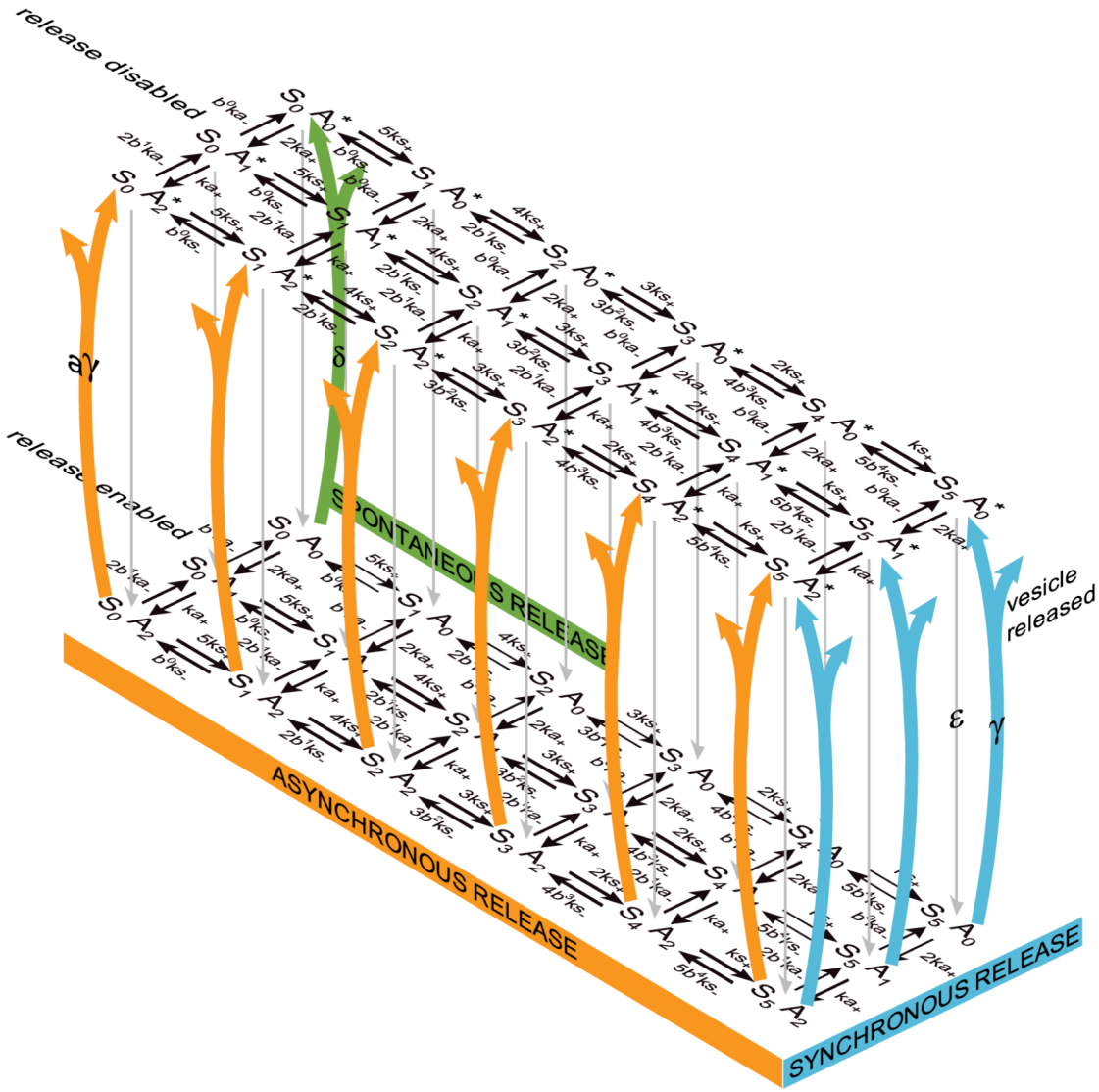

Figure 2.3: Calcium binding to synchronous and asynchronous sensor leading to vesicular release. The synchronous sensor (S) has five calcium binding sites, while the asynchronous sensor (A) has only two. The two pathways have distinct neurotransmitter release rates, with the synchronous release rate (γ) being faster than the asynchronous release rate ($a\gamma$). Figure reproduced from Nadkarni et al. (2010).

2.0.2 Measurement of release probability and mEPSC frequency

Changes in the number of VDCCs, their positions, and the RRP size in the model were done as required. Cytosolic calcium concentration equilibrates to 100nM in the model. Changes in calcium concentration are made in the reduced version of the model, which excludes the ion transporters and buffers, and maintains the presynaptic calcium concentration at a defined level. For mEPSC frequency simulations, since it involves few releases, the refilling of vesicles was turned off to avoid excess refilling.

To measure the release probability, 1000-5000 trials for a model configuration were performed. Lesser trials were required for configurations with high release probabilities. The release probability was calculated by taking the ratio of the number of trials with at least one vesicle release within 20 ms after initiation of the action potential to the total number of trials. 20ms inter-spike interval was used for the paired-pulse protocol. For train stimulus, pulse with 20Hz frequency were given for 1s.

For the mEPSC frequency measurements, 1000 trials of 2 sec each, without stimulus, were performed, and the frequency of vesicle release was calculated.

The simulations were performed in the high-performance computing cluster housed in IISER Pune.

2.0.3 Reduced model of short-term plasticity at CA3 presynapse

To simulate vesicular release activity at the CA3-CA1 presynapse for prolonged stimulus, we used a mathematical model of short-term plasticity, as described in the study by Mahajan and Nadkarni (2020) (Fig. 2.4).

In the STP model, the per-vesicle release probability evolves over time based on the neuron's spiking history (eqn 2.1) Following each spike, per-vesicle release probability (p_v) increases by an amount proportional to the facilitation parameter (α_f). The factor $(1 - p_v)$ makes sure that the probability doesn't exceed one. The exponential relaxation of p_v to its baseline level in the absence of the firing activity is described by the first term of the equation. The synaptic release probability (P_s) is related to the vesicular release probability (p_v) with the equation 2.2. Depression of the synaptic release probability happens due to

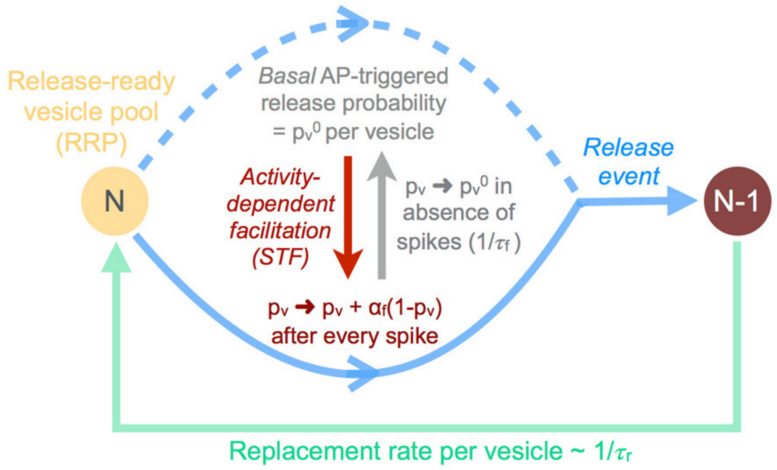

Figure 2.4: Modelling short-term plasticity. Vesicles are released with a per-vesicle release probability, p_v^0. With every spike, per-vesicle release probability increments with a value proportional to the facilitation parameter, α_f. In the absence of activity, p_v^0 approaches its baseline value exponentially, with time constant τ_f. The released vesicles are recovered stochastically with a mean recovery timescale of τ_r per vesicle. Reprinted from Mahajan and Nadkarni (2020).

the depletion of the readily releasable pool.

$$\frac{dp_v}{dt} = \frac{(p_v^0 - p_v)}{\tau_f} + \alpha_f(1 - p_v)\sum_i \delta(t - t_i) \tag{2.1}$$

$$P_s = 1 - (1 - p_v)^{N_{RRP}} \tag{2.2}$$

2.0.4 Measurement of Information transfer and energy use

Information rate and specific cost of information were calculated using the protocol as used by Mahajan and Nadkarni (2020). The parameters of the STP model were estimated for each configuration to capture its short-term plasticity profile. The basal per-vesicle release probability was calculated from the synaptic release probability measured with the spatially-explicit model using the equation 2.2. For each configuration, simulations with the paired-pulse stimulus were performed with the corresponding vesicular release probability, and the

α_f value that resulted in the paired-pulse ratio closest to the value was chosen.

For the info-energy measurements, the input signal mimicking the naturally occurring firing activity of the CA3 neuron is used. It's zero everywhere except when the mouse passes the neuron's place field. The passes are assumed to be for a constant time, and the frequency of each pass is assumed to have a Poisson distribution with a mean of 30 Hz.

To measure information transfer during vesicular release, we quantify how well the vesicle code represents the firing activity of the neuron. We calculate the average mutual information rate (R_{rs}), which measures the statistical relatedness of two variables. To normalize the differences in input signals, we reported the values of the relative mutual information rate, $R_{info} = R_{rs}/R_s$, where R_s is the information content of the input signal.

To assess the energy efficiency for each synaptic configuration, we computed the specific cost of information, $E = R_{ves}/R_{info}$, where R_{ves} is the average rate of vesicle fusion events. The metric represents the energy consumed per bit of information transmitted, with lower values indicating greater energy efficiency.

Chapter 3

Results & Discussion

3.1 Regulation of synaptic strength through homeostatic changes in VDCC expression and placement

An increase in RRP size and Ca flux through Voltage-Dependent Calcium Channels following activity suppression by TTX in hippocampal cultures has been reported by multiple studies (Thiagarajan et al., 2005; Han and Stevens, 2009; Zhao et al., 2011; Jeans et al., 2017). These presynaptic modifications help achieve homeostasis by influencing the probability of neurotransmitter release and thereby affecting the strengths of the synapses. An increase in the number of molecules in the VDCC nanodomains near the AZs, the fluorescence intensity of free molecules relative to the nanodomains intensity, and the number of free molecules near the AZ was observed after 24hr TTX treatment of hippocampal cultures in the research conducted by Netrakanti and Nair (2021). We investigate how each of these factors influences the probability of neurotransmitter release.

To study how the number of Ca channels in the **VDCC nanodomains** affects release probability, we make modifications in our CA3-CA1 synapse vesicular release model and measure release probabilities accordingly. Specifically, we place a single VDCC nanodomain of 50 nm radius at varying distances from the release site and quantify the effect of increasing VDCC number on release probability for each of the coupling distances. The 50 nm radius of the nanodomain is in agreement with the experimental data collected by Netrakanti and Nair (2021) for the hippocampal cultures.

Figure 3.1 shows the relationship between the release probability and the number of molecules in the nanodomain, with nanodomains located at a distance of 10nm - 400nm from the release site. The dependence of pr on the number of VDCCs is a sigmoid relationship, exhibiting a steeper curve for nanodomains placed closer to the release site.

While there exists a wide range of coupling distances in hippocampal neurons, the research by Nadkarni, Suhita, and colleagues demonstrates loose coupling in CA3-CA1 synapses, and predicts coupling distances to be in the range of 250-350 nm (Nadkarni et al., 2012). The magnitude by which the VDCC number change during homeostasis would, presumably, depend on the circumstances. According to the study conducted by Netrakanti and Nair (2021), the number of VDCCs in the nanodomains increase to upto approx. 1.5 their initial value, while the overall VDCC fluorescence intensity increases to upto approx. double its initial value after 24-hr TTX treatment of hippocampal neurons. Fig 3.2 A shows

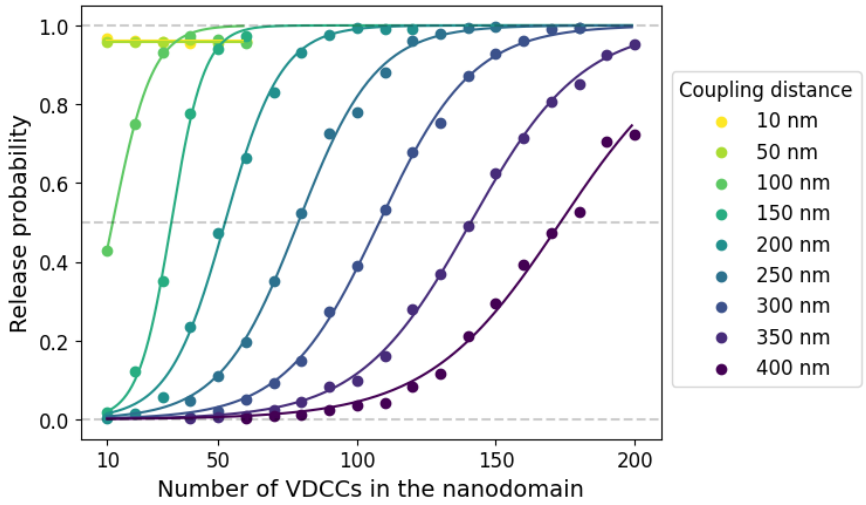

Figure 3.1: Relationship between the release probability and the number of clustered VDCCs. The dependence of the release probability on the number of VDCCs in the nanodomain is shown for various coupling distances, for VDCCs placed in a nanodomain of radius 50 nm.

the dependence of release probability (pr) on the number of VDCCs in the nanodomain for a coupling distance of 200 to 400 nm, for an increase in VDCC number to double its initial value.

To study how the probability of release changes on increasing the number of **free VDCC molecules**, we now disperse the channels in a region surrounding the release site with a given average distance. The coordinates of the molecules are selected randomly from a uniform distribution for each parameter set. To be able to compare with the results for the VDCCs arranged in a nanodomain, we measure pr for the same range of VDCC numbers and coupling distances as in the previous simulation (Fig 3.2 B). We see a general increase in pr for randomly spread configuration for the same average distance and number of VDCCs. The dependence of pr on VDCC number and coupling distance for free VDCCs appears to be noisy.

The results highlight the importance of the precise positioning of VDCC molecules, rather than just the average distance, in deciding the release probability. When VDCCs are dispersed within an area surrounding the release site, some are located in close proximity while others are further away, as compared to when they are all clustered at the same distance. The different release probabilities for the two placements may be attributed to the buffering of calcium by calbindin as it enters via the VDCCs. This also explains the apparent noise

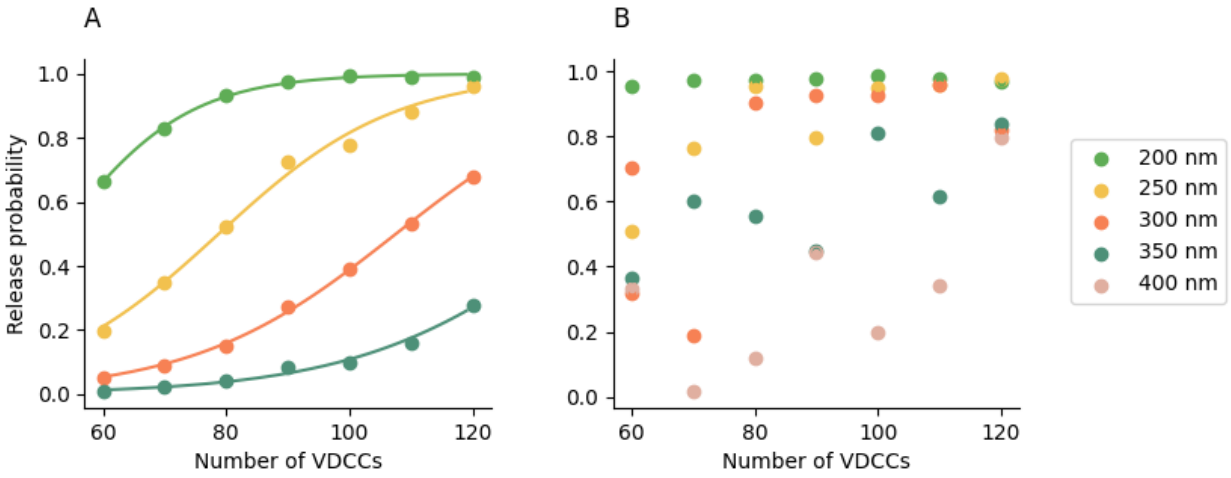

Figure 3.2: Variation of release probability with the number of VDCCs for (A) VDCCs clustered in a nanodomain of radius 50 nm placed at distances 200-350 nm from the release site, (B) VDCCs dispersed in a region with mean distances 200-400 nm from the release site.

observed in the pr measurements for the spread-out distribution. Even a few molecules in close proximity to the release site can have a considerable impact on the release probability.

3.1.1 Multiplicative scaling of VDCCs, and release probability

Multiplicative scaling of the VDCCs' average fluorescence intensity per synapse has also been observed following 24hr-TTX treatment in the study conducted by Netrakanti and Nair (2021). It remains unclear how such a coordinated change in VDCC expression might regulate synaptic strength in an attempt to achieve homeostasis.

We investigate how synaptic strengths change after multiplicative scaling of VDCC numbers in a population of CA3-CA1 synapses. We study the effects of multiplicative scaling for the VDCCs clustered in a single nanodomain. To identify any differences in response to scaling because of RRP size and coupling distance, we consider synapses with small and large RRP sizes (RRP = 5, 15) and sufficiently different coupling distances (200 nm, 300 nm). We get four synaptic configurations obtained from the combination of different RRP sizes and coupling distances. For each of the configurations, the appropriate number of VDCCs are considered in the synapses to have the whole variation in release probability (Fig 3.3).

Fig 3.4 displays the relationship between the release probabilities of synapses before

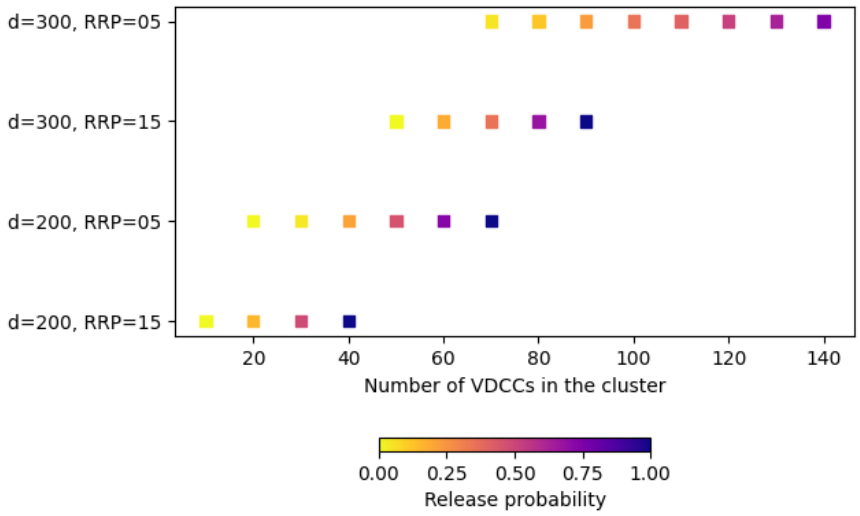

Figure 3.3: Configurations of the synaptic population for multiplicative scaling. For each combination of coupling distance (200 nm, 300 nm) and RRP size (5, 15), an appropriate range of VDCC number is considered in the initial population to capture a the range of release probability.

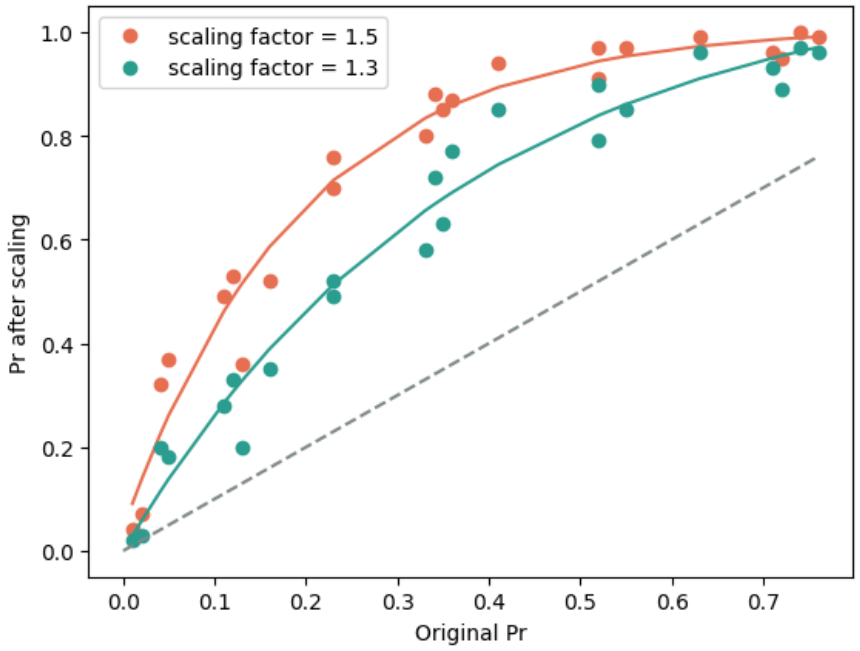

Figure 3.4: Effect of multiplicative scaling of VDCCs on the release probability. The probability of synapses after scaling is plotted against the original probability. The dashed line represents y=x.

and after the multiplicative scaling of VDCCs located in a single nanodomain. Fig 3.5 shows the same relationship with each configuration color coded differentially to make them distinguishable. The change in release probability due to scaling appears to depend mainly on the release probability prior to scaling, irrespective of the coupling distance or the RRP size of the synapse.

To examine the relationship more carefully and test whether the multiplicative scaling of VDCCs is causing additive/multiplicative scaling of synaptic strengths, we check the additive and multiplicative factors by which pr has changed after the scaling (Fig 3.5). We observe that the additive factor increases with the initial release probability until it saturates. Additionally, smaller scaling factors result in smaller additive factors, and saturation occurs for larger release probabilities. The multiplicative factors, on the other hand, decrease with pr. Small pr values have larger multiplicative factors, despite having smaller additive factors due to their small magnitude. The observations suggest that the probability of neurotransmitter release doesn't change by a constant additive/multiplicative factor after multiplicative scaling of VDCCs.

3.2 Effect on Short Term Plasticity as a consequence of presynaptic homeostatic modifications

Presynaptic modifications during homeostasis can have an impact on short-term plasticity at synapses. An inverse relationship between the release probability and paired-pulse ratio, a measure of short-term plasticity, has been observed in hippocampal synapses (Manabe et al., 1993; Debanne et al., 1996; Dobrunz and Stevens, 1997). Larger release probabilities tend to deplete vesicles and are associated with a lower paired-pulse ratio. Changes in readily releasable pool size and calcium flux through VDCCs are commonly observed presynaptic modifications following activity manipulation in vitro. We examine the effect of changes in VDCC expression and placement, and readily-releasable pool size on short-term plasticity.

Nadkarni and colleagues, in a study using the spatially explicit, stochastic, biophysical model of the CA3-CA1 presynapse, show that VDCCs must cluster at a distance of 250-350 nm in CA3-CA1 synapses to match the experimentally observed STP data. Our simulations are done for the same range of coupling distances.

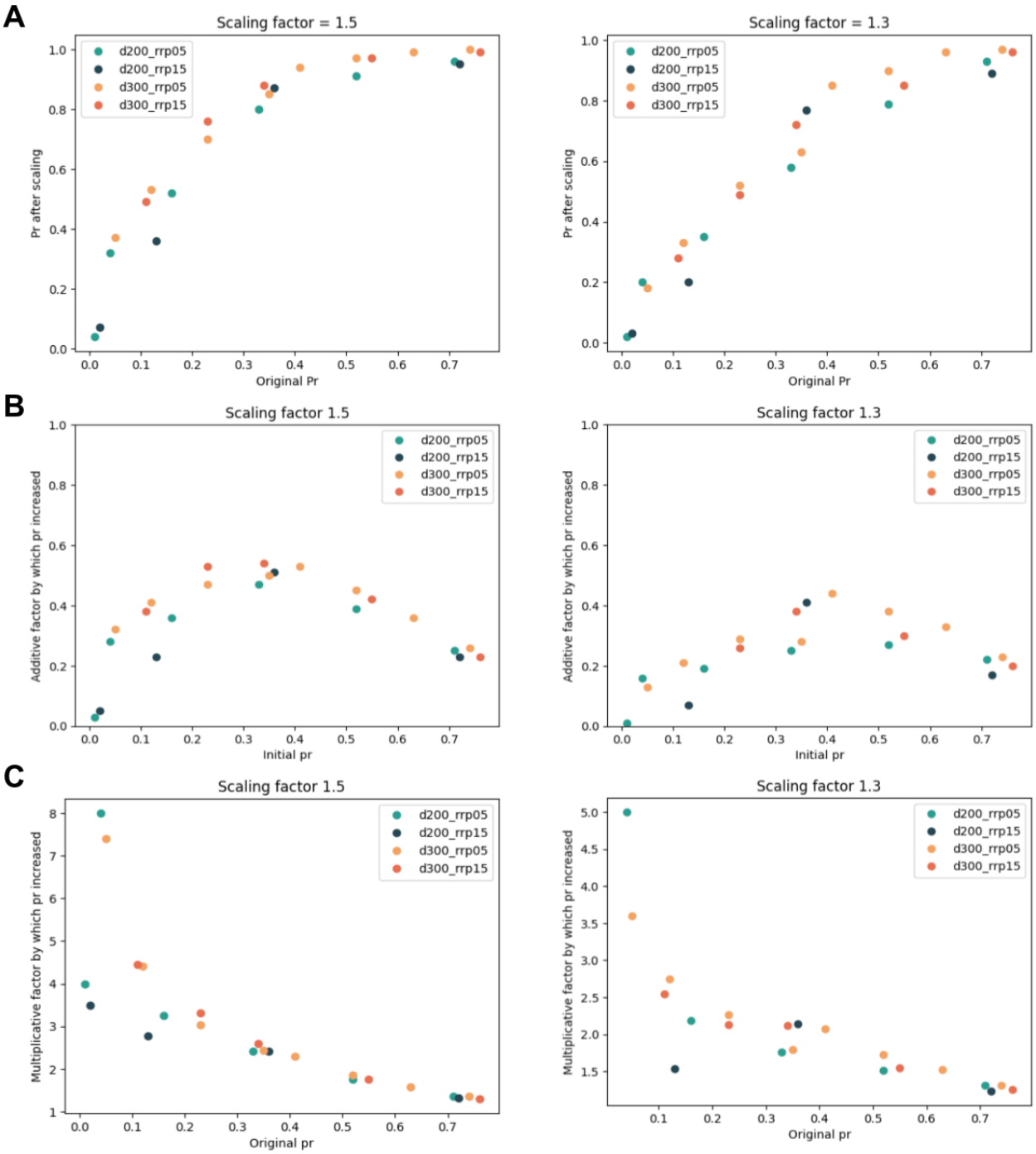

Figure 3.5: Effect of multiplicative scaling of VDCCs on the release probability: (A) Relationship between the release probability before and after the scaling, (B) Additive factors and (C) Multiplicative factors by which the release probabilities changed after the scaling.

3.2.1 Response to the paired-pulse stimulus

Fig 3.6 A and Fig 3.6 B show the variation in release probability and Paired-Pulse Ratio (PPR) with the number of clustered VDCCs and the free VDCCs respectively. As pr increases with the number of channels in the nanodomains, PPR becomes lower (Fig 3.6 A). Interestingly, this observation doesn't extend to the free VDCC molecules. PPR remains about one regardless of the number of free molecules and their placement (Fig 3.6 B). This shows that free VDCCs do not contribute to the residual calcium due to the first spike. It

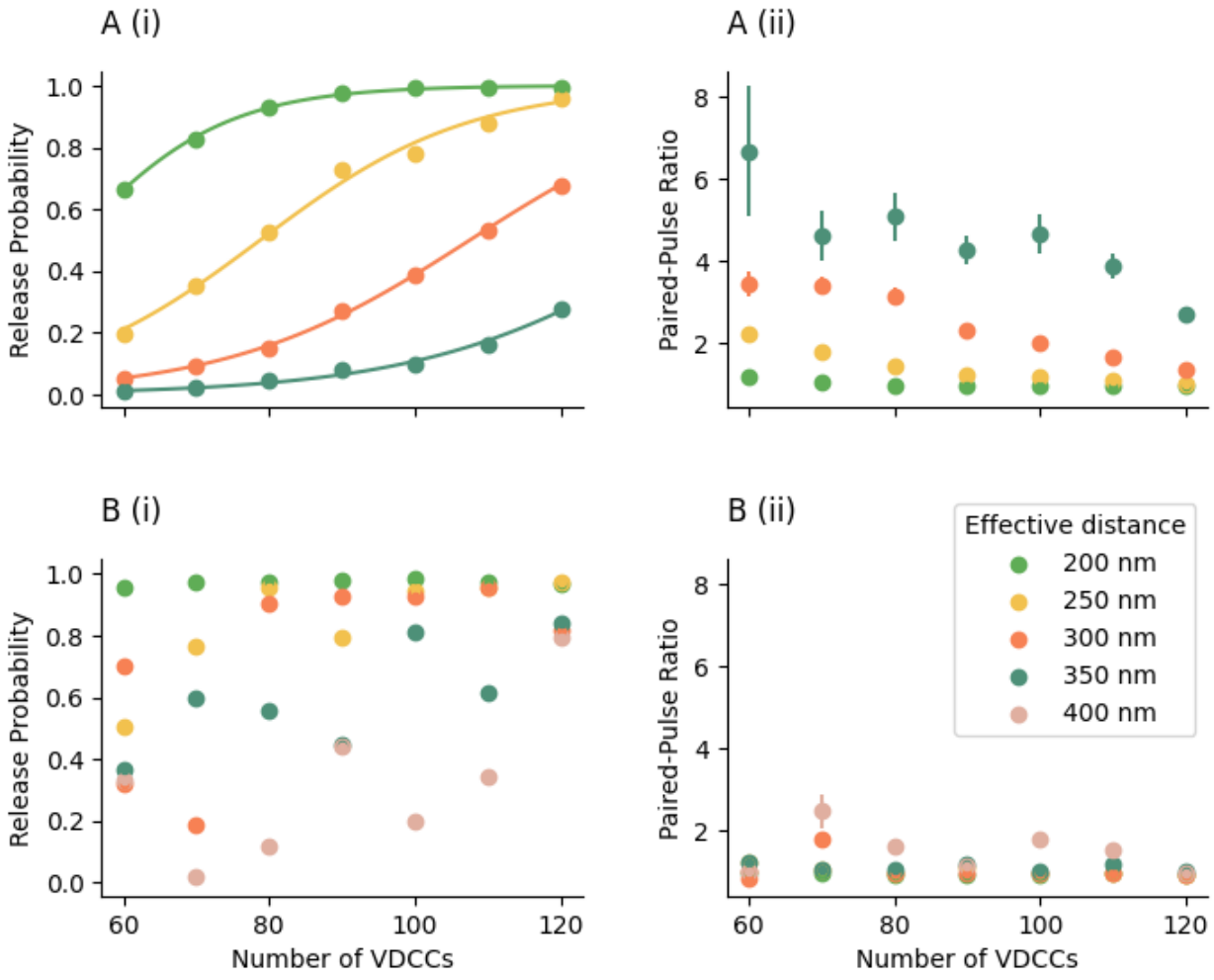

Figure 3.6: Variation of release probability and paired-pulse ratio with the number of VDCCs for (A) VDCCs clustered in a nanodomain of radius 50 nm placed at distances 200-350 nm from the release site, (B) VDCCs dispersed in a region with mean distances 200-400 nm from the release site.

can be explained by the buffering action of calbindin. When the molecules are placed farther apart from each other, the incoming calcium can get easily buffered by calbindin.

Studies on hippocampal cultures report around 25% increase in RRP size for 1-day TTX treatment and about a 35% increase when the treatment is given for 2 days. Fig 3.7 shows the dependence of pr and paired-pulse ratio on readily releasable size for about 40% increase in the value, for 60 VDCCs clustered in a nanodomain. The effect of RRP size on PPR appears weak, as compared to the effect due to an increase in clustered VDCCs. To further examine the magnitude of the effect homeostatic change in RRP size can have on PPR, we study the effect of increasing RRP size for different initial configurations of synapses. The VDCCs are clustered in a nanodomain, and for different VDCC numbers, coupling distances, and initial RRP sizes, giving the whole range of initial release probabilities, we increase the RRP size to around 50% the initial value (Fig 3.8). The data suggests that changes in RRP size have a feeble effect on the Paired-Pulse Ratio for a magnitude of change associated with presynaptic homeostasis.

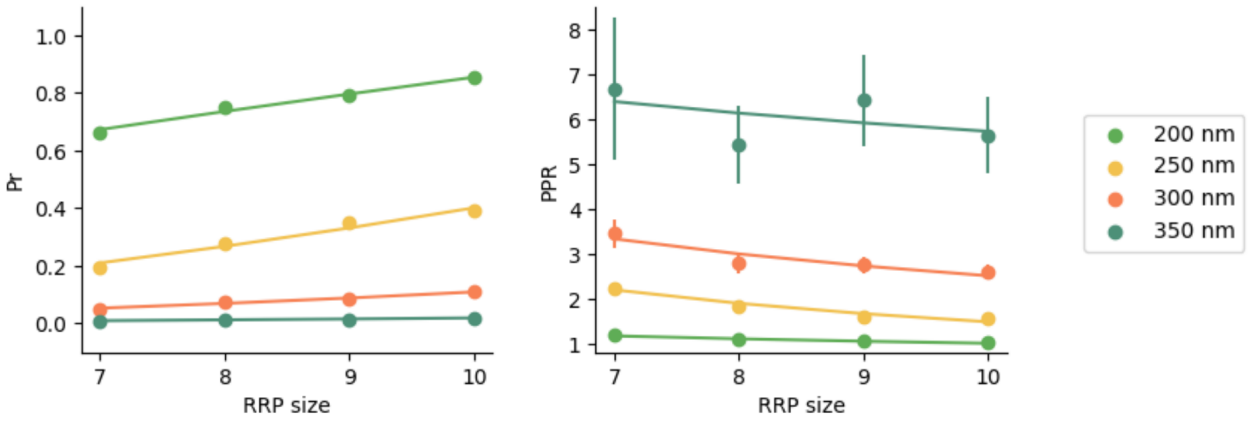

Figure 3.7: Variation of release probability and paired-pulse ratio with the readily-releasable pool size, for 60 VDCCs clustered at various distances from the release site.

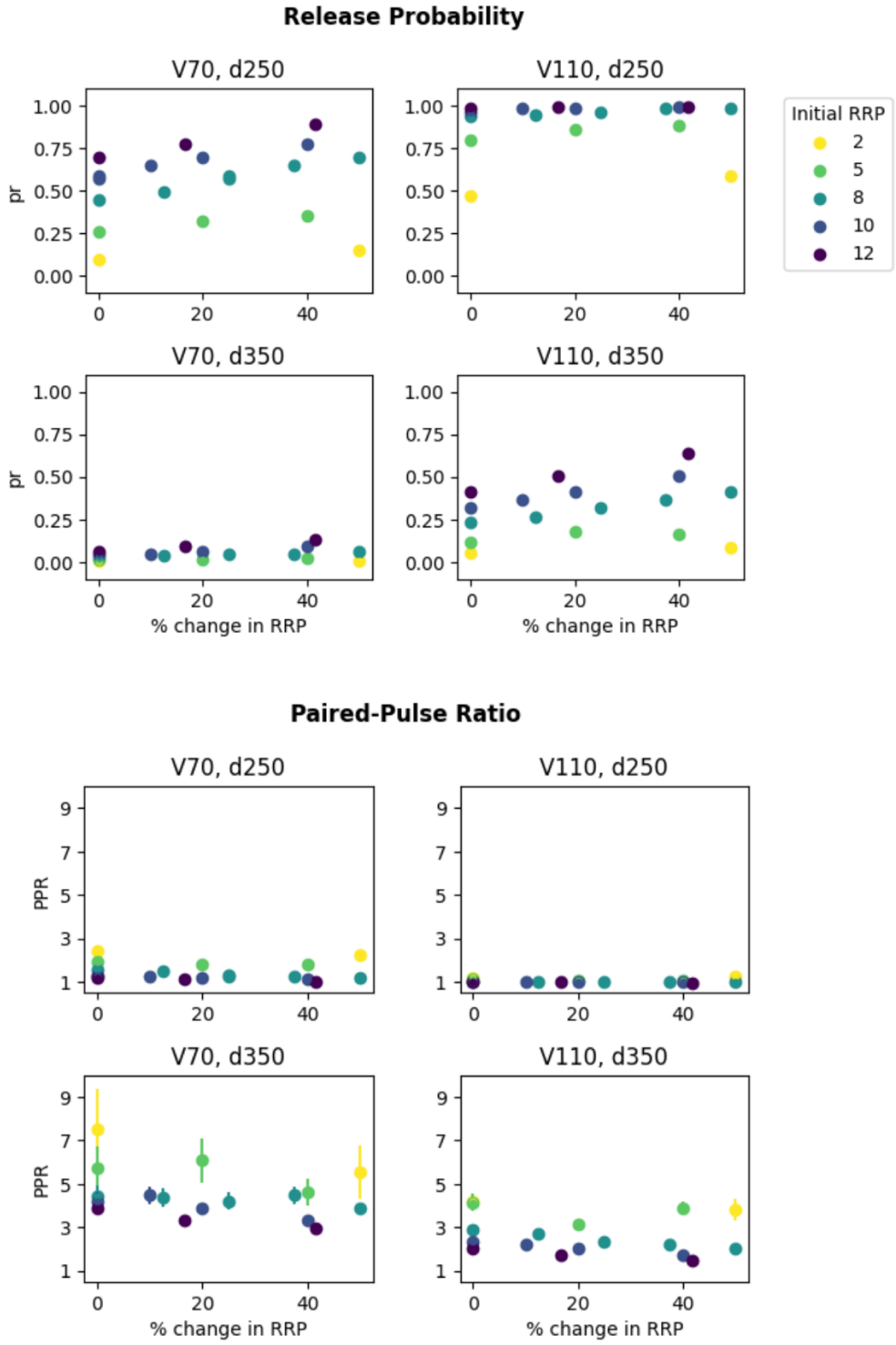

Figure 3.8: Effect of increasing RRP size on the paired-pulse ratio. For each combination of VDCC number (70, 110) and coupling distance (250 nm, 350 nm), RRP is increased to upto 50% its value for RRP sizes 2-12. Variation in release probability and paired-pulse ratio with changes in RRP is shown for each configuration.

3.2.2 Response to the spike train

To further examine the influence of presynaptic modifications on STP, we study the effect of changes in the number of clustered VDCCs and RRP size on the variation of release probability throughout a pulse train (Fig 3.9).

The results suggests that changes in the number of VDCCs has a considerable effect on the probability of transmission of each pulse of the spike train (Fig 3.9 A). As the number of channels increases, the release probability for the first pulse increases, and with that the RRP is depleted more rapidly, leading to a faster decrease in pr. This affects how the spike train is transmitted to the postsynaptic neuron.

For increase in RRP size, there seems to be an about uniform increase in the probability of transmission of each spike of the pulse train (Fig 3.9 B). The effect on the transmission of the spike train doesn't appear as drastic as for the change in the number of clustered VDCCs.

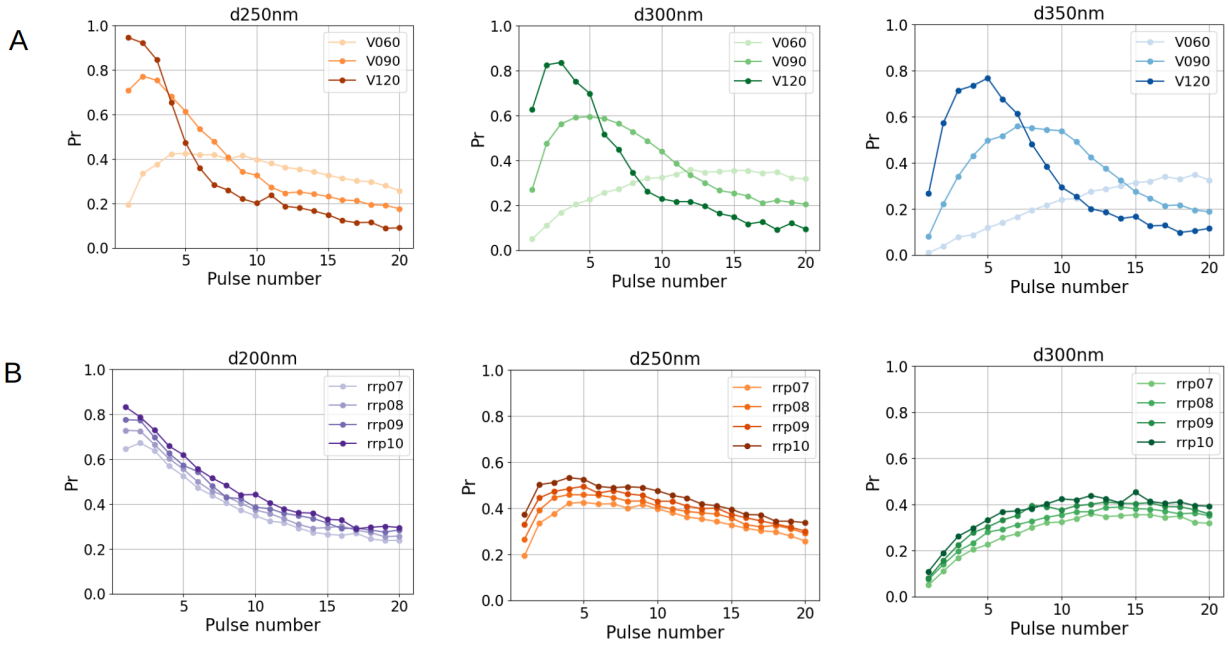

Figure 3.9: Effect of changing VDCC number and RRP size on short-term plasticity over a prolonged stimulus. Response to a second long 20 Hz stimulus for (A) different number of VDCCs in the nanodomain, (B) different RRP sizes. The effect of each is studied for multiple coupling distances.

3.3 Energy-Information Trade-off at synapses during presynaptic homeostasis

A crucial role of STP during information transmission at synapses was revealed in a study by Mahajan and Nadkarni (2020) using the computational modeling approach. They examined information transfer and energy use during transmission for synapses with different vesicular release probabilities and RRP sizes for various degrees of facilitation. Information transfer was enhanced in the presence of facilitation, and was independent of vesicular release probability as opposed to when there was no facilitation. They also showed that short-term plasticity in biological synapses maximizes information transfer in a cost-effective manner. Given that STP is altered during presynaptic homeostasis, we investigate the effect of presynaptic modifications such as changes in the number of clustered VDCCs and RRP size on information transfer and energy consumption during transmission.

We quantify information rate and energy efficiency for various configurations of the CA3-CA1 synapse using a methodology similar to that followed by Mahajan and Nadkarni (2020). The vesicular release activity for naturally occurring firing patterns of CA3 neuron is simulated using a reduced kinetics model of per-vesicle release probability. The parameters that determine the short-term plasticity profile in the model are estimated for each configuration, from the pr and PPR values obtained from the spatially-explicit biophysical model. The obtained parameters are used in the short-term plasticity model to simulate the presynaptic release activity for each configuration over a large time scale.

The simulations are performed for a coupling distance of 250-300 nm, with the VDCCs clustered placed in a nanodomain. For each coupling distance, a broad range of number of VDCCs in the nanodomain is considered for RRP size 2-17 to capture the whole range of release probabilities.

3.3.1 Interpretation of alterations in the short-term plasticity with the STP model

The short-term plasticity model developed by Mahajan and Nadkarni (2020) describes the vesicular release activity at the CA3-CA1 presynapse in response to a given firing pattern.

For each synaptic configuration, we find the corresponding initial per-vesicle release probability and facilitation parameter that defines the evolution of pv over time in the STP model. The observed changes in the short-term plasticity can now be described with changes in the new parameters.

Fig 3.10 shows the variation of basal per-vesicle release probability and facilitation parameter with the number of clustered VDCCs, RRP size, and coupling distance. Vesicular release probability increases with the number of VDCCs in the nanodomain and decreases with coupling distance, with minimal dependence on the RRP size. The facilitation parameter also increases with the VDCC number, and decreases with coupling distance, with minimal dependence on the RRP size.

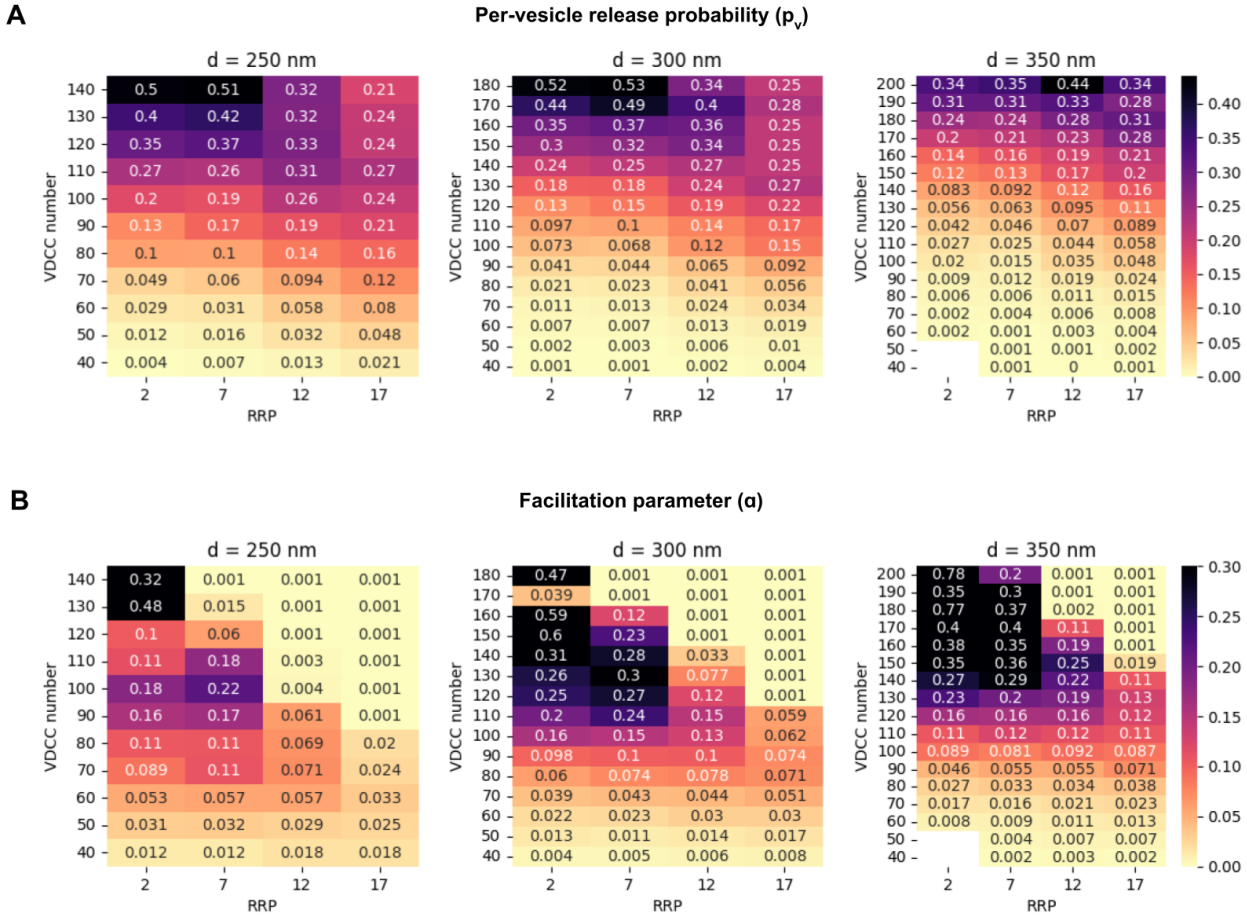

Figure 3.10: Variation of the parameters of the short-term plasticity model with VDCC number, RRP size and coupling distance: (A) per-vesicle release probability calculated from the synaptic release probability for each configuration, and (B) facilitation parameter estimated from the basal release probability and the paired pulse ratio.

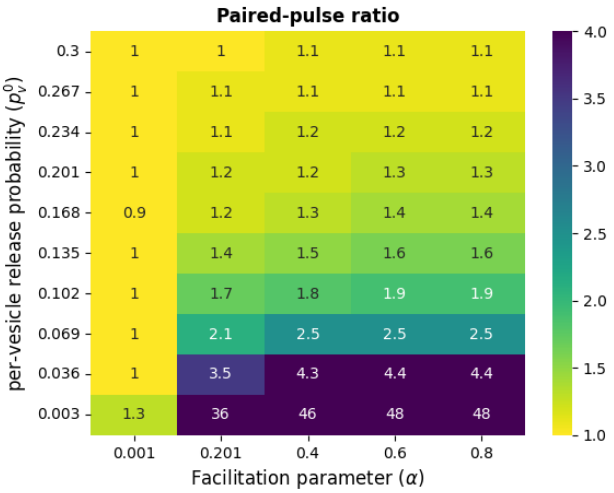

Figure 3.11: Dependence of paired-pulse ratio on the model parameters, per-vesicle release probability, and the facilitation parameter.

The dependence of PPR on vesicular release probability and the facilitation parameter from the simulation results with the STP model is shown in Fig 3.11. PPR exhibits significant sensitivity to the per-vesicle release probability, decreasing with an increase in the per-vesicle release probability and a decrease in the facilitation parameter.

Increasing the number of VDCCs leads to an increase in vesicular release probability and the facilitation parameter. As the previous data suggests, it also results in higher synaptic release probability and lower paired-pulse ratio. The decline in PPR subsequent to VDCCs increase is explicable by the heightened per-vesicle release probability due to the increased calcium flux. Similarly, the decline in PPR due to an enlarged RRP or a shorter coupling distance can be attributed to a higher per-vesicle release probability.

3.3.2 Analysis of the information rates and energy efficiency following presynaptic modifications

Fig 3.12 A shows the heatmap of relative mutual information rate (R_{info}) with RRP size, VDCC number, and coupling distance as variables. Interestingly, R_{info} remains almost constant with changes in the number of VDCCs across all RRP sizes and coupling distances. Similarly, it remains constant for different coupling distances but increases with RRP size. For smaller readily-releasable pool sizes, a lower information rate presumably results because

of the resource constraints owing to the quicker depletion of vesicle pools during transmission. However, for the magnitude of RRP size changes associated with homeostatic plasticity, there won't be a considerable influence on the information transfer. The results suggest that information transfer is robust to homeostatic modifications.

The heatmap in fig 3.12 B displays the variation of the specific cost of information with RRP size, coupling distance, and number of VDCCs. With an increase in the number of VDCCs, the specific cost of information becomes stable after increasing briefly. It's greater for shorter coupling distances and larger RRP sizes. The data suggests that energy efficiency, the inverse of the specific cost of information, varies with changes in VDCC numbers and RRP size.

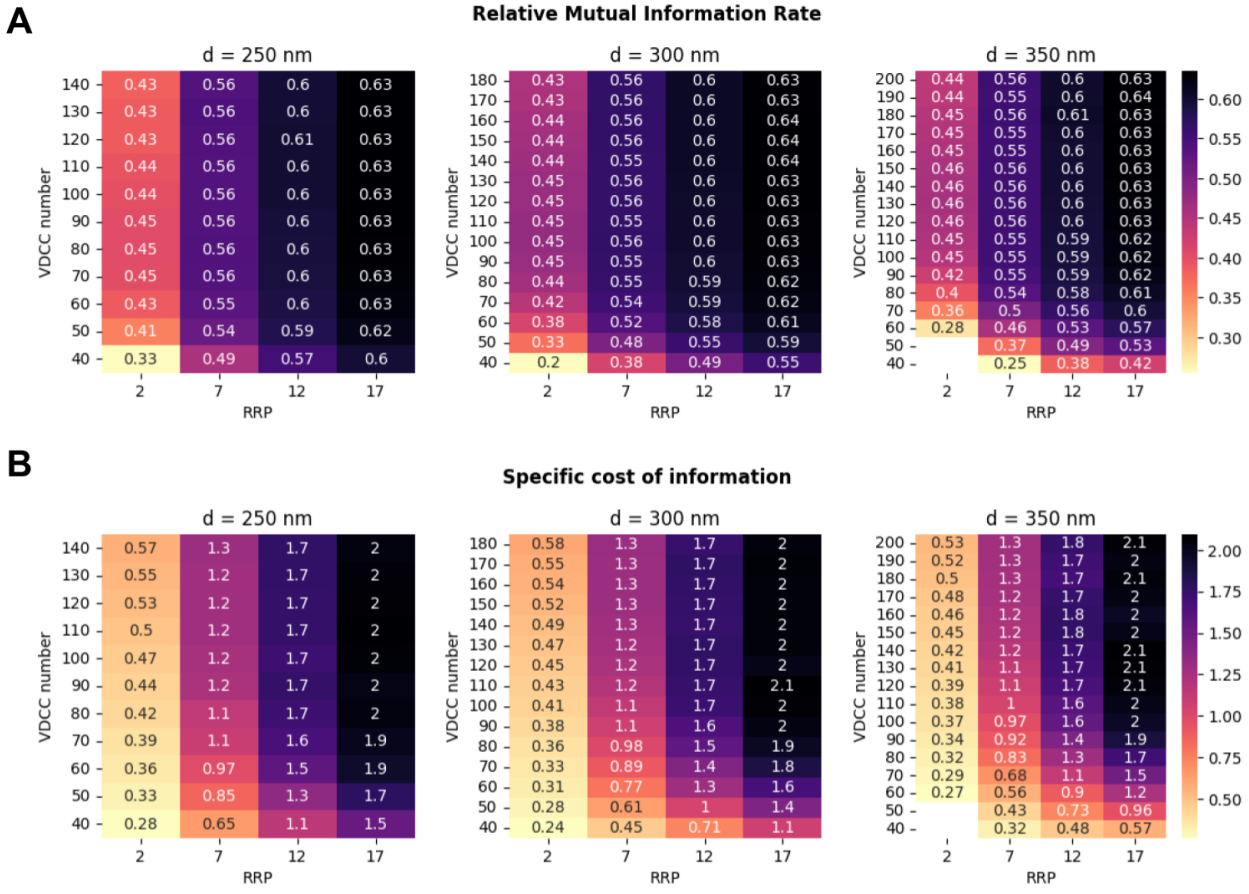

Figure 3.12: Variation of (A) Relative Mutual Information Rate (R_{info}), and (B) Specific cost of information (E), with the number of VDCCs in the nanodomain, RRP size, and coupling distance.

3.4 Uncovering the drivers of changes in mEPSC frequency following presynaptic homeostasis

Several studies have reported increased mEPSC frequency following activity suppression in hippocampal cultures. The increase in frequency is about twice or thrice its initial value, depending on various factors (Han and Stevens, 2009; Thiagarajan et al., 2005; Wierenga et al., 2006). We investigate the potential drivers of changes in mEPSC frequency by examining its dependence on various synaptic parameters.

3.4.1 A proportional increase in mEPSC frequency with RRP size

Increase in RRP size is considered one of the significant reasons for the increase in mEPSC frequency. Studies report approximately a 25%-35% increase in RRP size after in vitro suppression of activity in hippocampal synapses, with a corresponding 100%-200% increase in mEPSC frequency (Han and Stevens, 2009; Thiagarajan et al., 2005).

To check the dependence of mEPSC frequency on RRP size, we measure the frequency for different RRP sizes for basal calcium concentrations of 100nM, 200nM, and 300nM (Fig 3.13 A). The results indicate that an increase in RRP size leads to a proportional increase in mEPSC frequency, regardless of the basal calcium concentration (Fig 3.13 B).

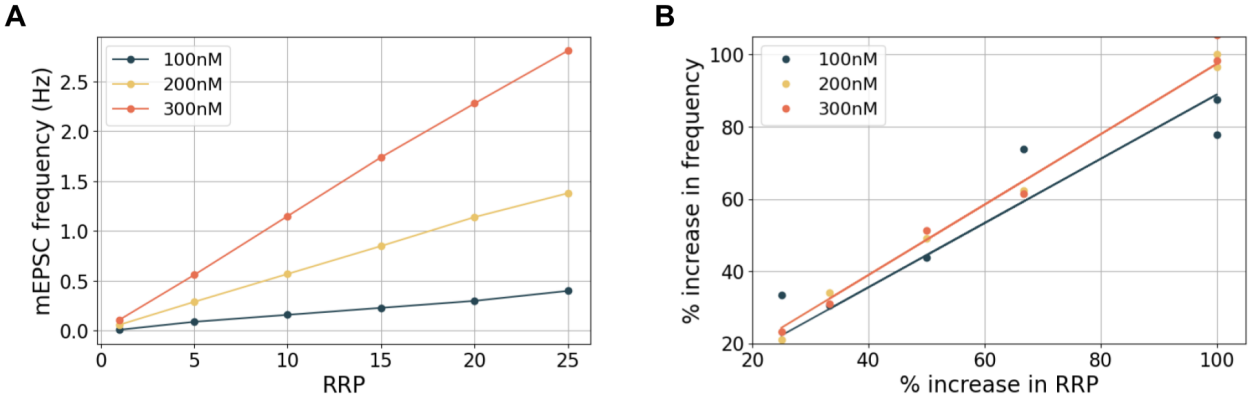

Figure 3.13: Effect of increasing RRP size on mEPSC frequency at different basal calcium concentrations in the presynapse.

The influx of calcium because of the stochastic opening of calcium channels present near

the release site might influence the relationship between the frequency and the RRP size. In order to check for this possibility, we ran the simulations with VDCCs close to the release site, with all the relevant ion channels and the calcium buffer in the model. VDCCs were dispersed in an area around the release site, with an average distance of 50 nm. Despite the proximity of the VDCCs to the release site, we do not observe a significant change in the relationship between RRP size and mEPSC frequency (Fig 3.14). It can be noted that the presynaptic Ca2+ concentration in these simulations equilibrates to about 100nM.

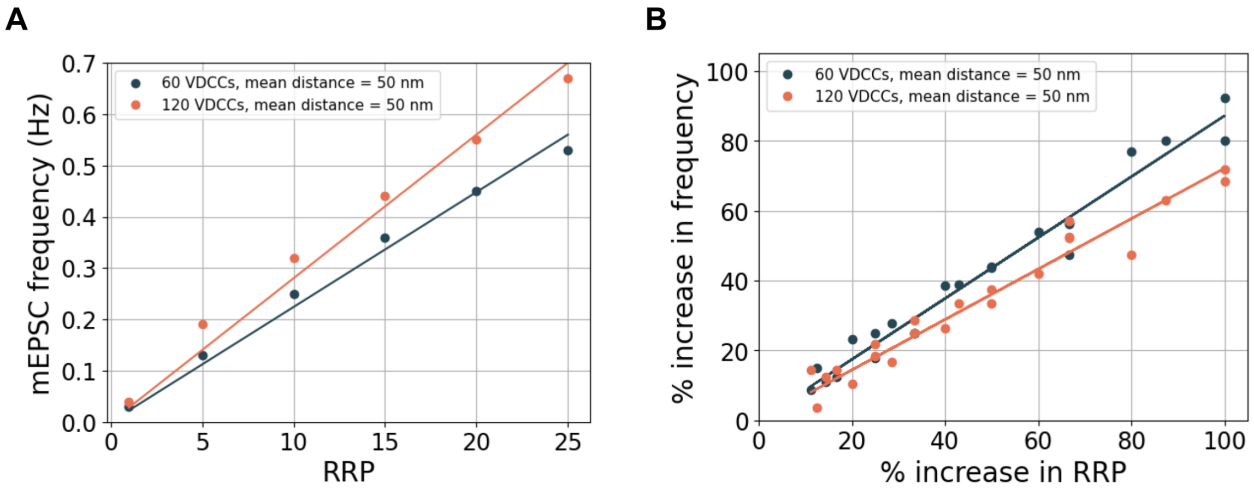

Figure 3.14: Effect of increasing RRP size on mEPSC frequency with VDCCs in proximity to the release site. The basal calcium concentration equillibriates to around 100 nM in these simulations.

A proportional increase in mEPSC frequency with the RRP size, as suggested by our data, leaves a major fraction of the increase in frequency unexplained. For instance, a 25% increase in RRP size following 1-day TTX treatment only accounts for a 25% increase in mEPSC frequency, for an observed increase of about 100%. For 2-day TTX activity blockage, RRP increase accounts only for about a 35% increase in frequency for an observed increase of 200%.

3.4.2 Calcium flux through VDCCs has a minor influence on the frequency

An increase in stimulus-induced calcium flux through VDCC has been observed after TTX treatment of hippocampal cultures (Jeans et al., 2017; Zhao et al., 2011). About a twofold in-

crease in the VDCCs' average fluorescence intensity was observed after 1-day TTX treatment of cultured hippocampal neurons, in the super-resolution microscopy study by Netrakanti and Nair (2021). With observed changes in the expression and organisation of VDCCs, we test whether calcium influx through the channels during the resting state might have an influence on the mEPSC frequency.

In the absence of a stimulus, we measured the average calcium concentration at the AZ with 100 VDCCs clustered at 200 nm from the release site and compared it with the concentration in the absence of the calcium channels. The calcium concentration remains about the same (Fig. 3.15). The calcium flux through VDCCs in the absence of stimulus is about three calcium ions per channel per second. The measured mEPSC frequency values for the two cases are 0.17 Hz and 0.16 Hz, respectively.

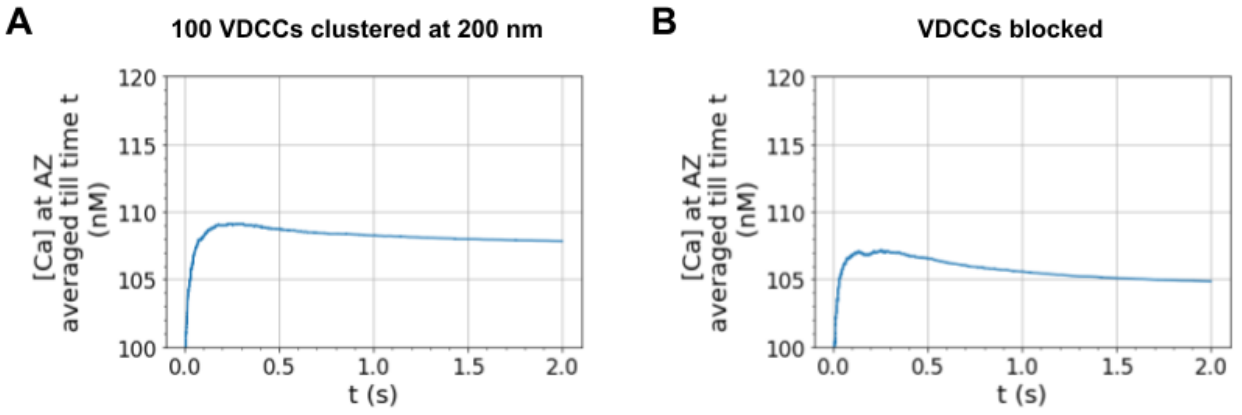

Figure 3.15: Effect of removing VDCCs on the calcium concentration at the active zone. Presynaptic activity for 2s is simulated without any stimulus. Calcium concentration at the active zone averaged over time is shown for two cases: (A) when 100 VDCCs are clustered at 200nm from the release site, and (B) when VDCCs are removed from the model (VDCCs blocked).

To further explore the influence of VDCCs on mEPSC frequency, we doubled their numbers with channels dispersed around the AZ and measured the frequencies accordingly. Doubling of channel numbers influences the frequency only for very short mean distances (Fig 3.16). Even then, the effect is only minor compared to the observed magnitude of changes.

The results suggest that VDCCs do not have a considerable influence on the calcium concentration at the active zone and the frequency of vesicle releases, in the absence of a stimulus.

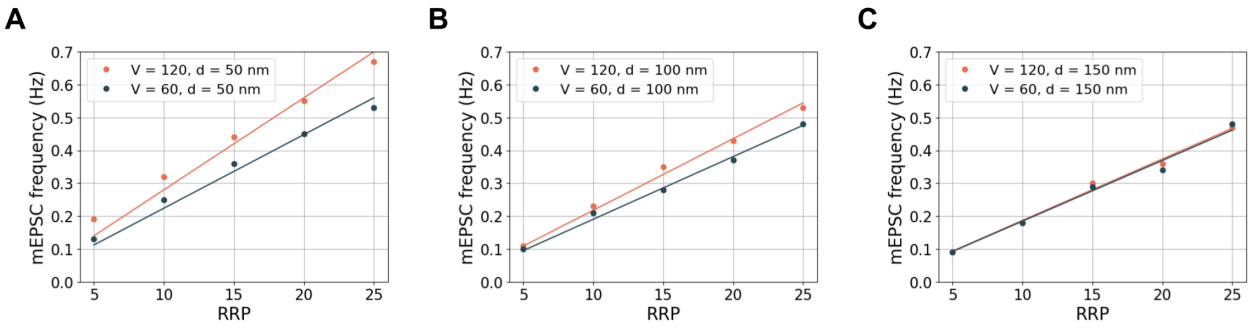

Figure 3.16: Effect of increasing the number of VDCCs on mEPSC frequency for various RRP sizes for VDCCs placed at a mean distance of (A) 50 nm, (B) 100 nm, (C) 150 nm.

3.4.3 mEPSC frequency is highly sensitive to basal Calcium levels

An increase in vesicle release in the absence of stimulus may be due to a rise in basal calcium levels. We check the dependency of mEPSC frequency on the presynaptic calcium concentration for various RRP sizes. An increase in the concentration from 100 nM to 200 nM leads to an approx three-fold increase in the frequency, with minimal dependence on RRP size (Fig. 3.17 A). Even a modest increase in the concentration from 100 nM to just 140 nM raises the frequency to approx. double its initial value (Fig. 3.17 B).

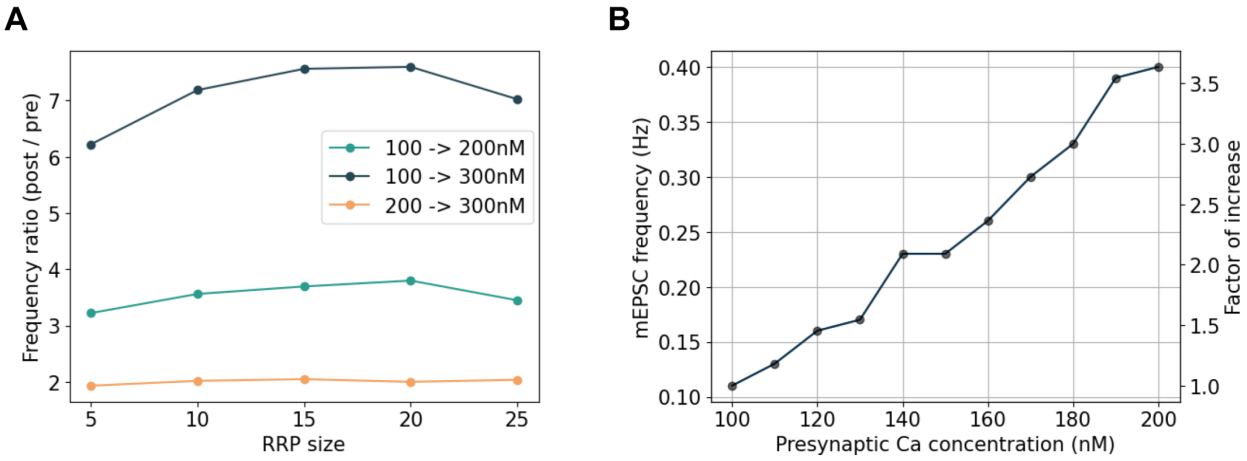

Figure 3.17: Change in mEPSC frequency with presynaptic basal calcium concentration. (A) Factor of increase on increasing the calcium concentration from 100 nM to 200 nM, 100 nM to 300 nM, and from 200 nM to 300 nM for various RRP sizes. (B) Dependence of mEPSC frequency on basal calcium concentration for RRP size = 7.

Overall, our analysis of mEPSC frequency explores the causal link for the increase in mEPSC frequency. Changes in RRP size are largely insufficient to account for the observed magnitude of the increase. Experimental studies have observed an elevated synapse density which could be responsible for the increase in mEPSC frequency, but there are several studies in which enhanced mEPSC frequency has been observed without changes in synapse density (Han and Stevens, 2009; Thiagarajan et al., 2005; Bacci et al., 2001). Our data suggests high sensitivity of mEPSC frequency to basal calcium concentration in the presynapse. In the absence of other apparent factors that might be responsible for the observed magnitude of changes, we suggest elevated basal calcium concentration to be a likely factor causing an increase in mEPSC frequency.

Chapter 4

Conclusion & Future Directions

Homeostatic plasticity maintains the average firing rate through a combination of various modifications. Even though it was discovered as a stabilizing mechanism, considering that it involves significant changes, it might have a more dynamic role in shaping neural activity. We investigated how homeostatic modifications at the presynapse affect the transmission of presynaptic neuronal firing activity.

We first examined how changes in the expression and placement of VDCCs affect the success of transmission of a single action potential. The probability of neurotransmitter release shows a logistic growth with the number of clustered VDCCs. With the number of free VDCCs, the variation is rather noisy because of the random positioning of the channels. Even when free VDCCs are placed with the same average distance as the clustered VDCCs, the release probability corresponding to free VDCCs can be influenced greatly by a few channels placed close to the readily-releasable pool. Given that synaptic strengths are often multiplicatively scaled during postsynaptic homeostasis, we identified the effect of multiplicative scaling of VDCCs on the neurotransmitter release probabilities of the synapses. The release probabilities do not change by a constant additive or multiplicative factor. The effect of such multiplicative scaling of VDCCs would also depend on the further processing leading to the generation of an action potential.

We studied the effect of homeostatic presynaptic modifications on short-term plasticity by examining the transmission of a paired-pulse and a train of action potentials. The paired-pulse ratio decreases with the number of clustered VDCCs as the release probability increases. When VDCCs are spread out, the paired-pulse ratio always remains one. This suggests that the free channels don't contribute to the residual calcium that leads to the rise in the release probability. We also interpreted the variations in the paired-pulse ratio with the number of clustered VDCCs using the short-term plasticity model. The lowered paired-pulse ratio for more channels results due to an increase in basal per-vesicle release probability rather than a weaker facilitation strength. Our simulations with the pulse train further suggest that changes in the number of clustered VDCCs and the RRP size affect the probability of neurotransmitter release over the pulses. The effect of RRP size is much less compared to the effect of VDCC number. The changes in short-term plasticity during homeostasis might have important implications given its crucial computational roles.

Since short-term plasticity has been shown to influence information transfer and energy efficiency during synaptic transmission, we measured their dependence on the number of

clustered VDCCs and the RRP size. With the homeostatic changes in VDCC number and RRP size, the relative mutual information rate remains almost constant. This suggests that, despite changes in short-term plasticity, the information transfer via vesicular release is unaffected by these modifications. However, the specific cost of information increases, i.e., the energy efficiency decreases with an increase in VDCC number and RRP size.

Additionally, we tried to explain the increase in mEPSC frequency observed after in vitro suppression of activity. Increased frequency of release without stimulus may result either from enlarged RRP or enhanced per-vesicle release rate. According to our results, mEPSC frequency increases proportionally with the RRP size and is only partly explained by it. Our data suggests high sensitivity of mEPSC frequency on the basal calcium concentration. In the absence of other factors to account for the large magnitude of changes in mEPSC frequency, we suggest that a plausible increase in basal calcium concentration could be responsible for the observed changes. The predicted changes in baseline calcium concentration are consistent with the observations of accelerated vesicular turnover following the suppression of activity (Bacci et al., 2001; Turrigiano and Nelson, 2004; Thiagarajan et al., 2005).

Our analysis of short-term plasticity has considered the effect of clustered VDCCs and free VDCCs separately. The calcium through free VDCCs gets easily buffered by calbindin but may saturate the buffers, leading to lesser buffering during the subsequent spikes. Studying with both clustered and free VDCCs together might give interesting results. The study also doesn't incorporate the effect of changes in baseline cytosolic calcium concentration. The impact on short-term plasticity during homeostasis, as examined in our study, and observed in several experiments, along with the postsynaptic modifications that occur during homeostasis, suggests a metaplastic role of homeostasis (Thiagarajan et al., 2005; Yee et al., 2017; Li et al., 2019). For instance, the study by Hobbiss and colleagues observed an altered Hebbian plasticity threshold and breakdown of input specificity following activity suppression in hippocampal neurons (Hobbiss et al., 2018). The computational modeling approach would also be a great tool for exploring how Hebbian thresholds are altered during homeostasis.

In summary, to understand the role of homeostatic plasticity in shaping neural activity, we developed a computational modeling framework to understand the effects of presynaptic homeostatic modifications. Short-term plasticity has important computational roles. Still, only a few experimental studies have measured alterations in short-term plasticity after homeostatic plasticity (Kim and Tsien, 2008; Soares et al., 2017; Delvendahl et al., 2019).

We examined the effects of homeostatic modifications on short-term plasticity and attempted to understand its implications. Many experimental studies have measured changes in mEPSC frequency as a proxy for presynaptic homoeostatic changes. But the reasons for enhanced mEPSC frequency were only partially understood. With our computational model, we could mechanistically explain the reasons for the experimentally observed increase in mEPSC frequency. Overall, our study gives valuable insights into how presynaptic homeostatic works and interacts with the other mechanisms that influence information processing at synapses.

Bibliography

L. F. Abbott and Sacha B. Nelson. Synaptic plasticity: taming the beast. *Nature Neuroscience*, 3(11):1178–1183, November 2000. ISSN 1546-1726. doi: 10.1038/81453. URL https://www.nature.com/articles/nn1100_1178. *Number* : 11*Publisher* : *NaturePublishingGroup*.

Alberto Bacci, Silvia Coco, Elena Pravettoni, Ursula Schenk, Simona Armano, Carolina Frassoni, Claudia Verderio, Pietro De Camilli, and Michela Matteoli. Chronic Blockade of Glutamate Receptors Enhances Presynaptic Release and Downregulates the Interaction between Synaptophysin-Synaptobrevin–Vesicle-Associated Membrane Protein 2. *Journal of Neuroscience*, 21(17):6588–6596, September 2001. ISSN 0270-6474, 1529-2401. doi: 10.1523/JNEUROSCI.21-17-06588.2001. URL https://www.jneurosci.org/content/21/17/6588. Publisher: Society for Neuroscience Section: ARTICLE.

Dominique Debanne, Nathalie C Guerineau, BH Gähwiler, and Scott M Thompson. Paired-pulse facilitation and depression at unitary synapses in rat hippocampus: quantal fluctuation affects subsequent release. *The Journal of physiology*, 491(1):163–176, 1996.

Igor Delvendahl and Martin Müller. Homeostatic plasticity—a presynaptic perspective. *Current Opinion in Neurobiology*, 54:155–162, February 2019. ISSN 09594388. doi: 10.1016/j.conb.2018.10.003. URL https://linkinghub.elsevier.com/retrieve/pii/S0959438818300436.

Igor Delvendahl, K. Kita, Katarzyna Kita, M. Mueller, and Martin F. Mueller. Rapid and Sustained Homeostatic Control of Presynaptic Exocytosis at a Central Synapse. *bioRxiv*, page 785535, September 2019. doi: 10.1101/785535. MAG ID: 2976986266.

Lynn E. Dobrunz and Charles F. Stevens. Heterogeneity of Release Probabil-

ity, Facilitation, and Depletion at Central Synapses. *Neuron*, 18(6):995–1008, June 1997. ISSN 0896-6273. doi: 10.1016/S0896-6273(00)80338-4. URL https://www.sciencedirect.com/science/article/pii/S0896627300803384.

Edward B. Han and Charles F. Stevens. Development regulates a switch between post- and presynaptic strengthening in response to activity deprivation. *Proceedings of the National Academy of Sciences*, 106(26):10817–10822, June 2009. ISSN 0027-8424, 1091-6490. doi: 10.1073/pnas.0903603106. URL https://pnas.org/doi/full/10.1073/pnas.0903603106.

Anna Felicity Hobbiss, Yazmin Ramiro-Cortés, and Inbal Israely. Homeostatic Plasticity Scales Dendritic Spine Volumes and Changes the Threshold and Specificity of Hebbian Plasticity. *iScience*, 8:161–174, October 2018. ISSN 2589-0042. doi: 10.1016/j.isci.2018.09.015. URL https://www.sciencedirect.com/science/article/pii/S2589004218301500.

Alexander F. Jeans, Fran C. van Heusden, Bashayer Al-Mubarak, Zahid Padamsey, and Nigel J. Emptage. Homeostatic Presynaptic Plasticity Is Specifically Regulated by P/Q-type Ca2+ Channels at Mammalian Hippocampal Synapses. *Cell Reports*, 21 (2):341–350, October 2017. ISSN 2211-1247. doi: 10.1016/j.celrep.2017.09.061. URL https://www.sciencedirect.com/science/article/pii/S2211124717313517.

Rex A Kerr, Thomas M Bartol, Boris Kaminsky, Markus Dittrich, Jen-Chien Jack Chang, Scott B Baden, Terrence J Sejnowski, and Joel R Stiles. Fast monte carlo simulation methods for biological reaction-diffusion systems in solution and on surfaces. *SIAM journal on scientific computing*, 30(6):3126–3149, 2008.

Jimok Kim and Richard W. Tsien. Synapse-Specific Adaptations to Inactivity in Hippocampal Circuits Achieve Homeostatic Gain Control while Dampening Network Reverberation. *Neuron*, 58(6):925–937, June 2008. ISSN 0896-6273. doi: 10.1016/j.neuron.2008.05.009. URL https://www.sciencedirect.com/science/article/pii/S0896627308004182.

Jie Li, Esther Park, Lei R. Zhong, and Lu Chen. Homeostatic synaptic plasticity as a metaplasticity mechanism—a molecular and cellular perspective. *Current Opinion in Neurobiology*, 54:44–53, February 2019. ISSN 0959-4388. doi: 10.1016/j.conb.2018.08.010. URL https://www.sciencedirect.com/science/article/pii/S0959438818301338.

Gaurang Mahajan and Suhita Nadkarni. Local Design Principles at Hippocampal Synapses Revealed by an Energy-Information Trade-Off. *eNeuro*, 7(5):ENEURO.0521–19.2020, September 2020. ISSN 2373-2822. doi: 10.1523/ENEURO.0521-19.2020. URL https://www.ncbi.nlm.nih.gov/pmc/articles/PMC7540928/.

TOSHIYA Manabe, DJ Wyllie, DAVID J Perkel, and ROGER A Nicoll. Modulation of synaptic transmission and long-term potentiation: effects on paired pulse facilitation and epsc variance in the ca1 region of the hippocampus. *Journal of neurophysiology*, 70(4): 1451–1459, 1993.

Kenneth D. Miller and David J. C. MacKay. The Role of Constraints in Hebbian Learning. *Neural Computation*, 6(1):100–126, January 1994. ISSN 0899-7667. doi: 10.1162/neco.1994.6.1.100. URL https://doi.org/10.1162/neco.1994.6.1.100.

Venkatesh N. Murthy, Thomas Schikorski, Charles F. Stevens, and Yongling Zhu. Inactivity produces increases in neurotransmitter release and synapse size. *Neuron*, 32(4):673–682, November 2001. doi: 10.1016/s0896-6273(01)00500-1. MAG ID: 2080611091.

Suhita Nadkarni, Thomas M. Bartol, Terrence J. Sejnowski, and Herbert Levine. Modelling Vesicular Release at Hippocampal Synapses. *PLOS Computational Biology*, 6(11): e1000983, November 2010. ISSN 1553-7358. doi: 10.1371/journal.pcbi.1000983. URL https://journals.plos.org/ploscompbiol/article?id=10.1371/journal.pcbi.1000983. Publisher: Public Library of Science.

Suhita Nadkarni, Thomas M Bartol, Charles F Stevens, Terrence J Sejnowski, and Herbert Levine. Short-term plasticity constrains spatial organization of a hippocampal presynaptic terminal. *Proceedings of the National Academy of Sciences*, 109(36):14657–14662, 2012.

Pallavi Rao Netrakanti and Deepak Nair. Role of calcium sensors in differential alignment of synaptic nanomachinery during neurotransmission. *in preparation and personal communication with Netrakanti, P, IISc*, 2021. URL https://etd.iisc.ac.in/handle/2005/5733?show=full.

Nishant Singh, Thomas Bartol, Herbert Levine, Terrence Sejnowski, and Suhita Nadkarni. Presynaptic endoplasmic reticulum regulates short-term plasticity in hippocampal synapses. *Communications Biology*, 4(1):1–13, February 2021. ISSN 2399-3642. doi: 10.1038/s42003-021-01761-7. URL

https://www.nature.com/articles/s42003-021-01761-7. Number: 1 Publisher: Nature Publishing Group.

Cary Soares, Kevin F. H. Lee, and Jean-Claude Béïque. Metaplasticity at CA1 Synapses by Homeostatic Control of Presynaptic Release Dynamics. *Cell Reports*, 21(5):1293–1303, October 2017. ISSN 2211-1247. doi: 10.1016/j.celrep.2017.10.025. URL https://www.sciencedirect.com/science/article/pii/S2211124717314572.

Joel R Stiles, Dirk Van Helden, Thomas M Bartol, Edwin E Salpeter, and Miriam M Salpeter. Miniature endplate current rise times¡ 100 μ s from improved dual recordings can be modeled with passive acetylcholine diffusion from a synaptic vesicle. *Proceedings of the National Academy of Sciences of the United States of America*, pages 5747–5752, 1996.

Joel R Stiles, Thomas M Bartol, et al. Monte carlo methods for simulating realistic synaptic microphysiology using mcell. *Computational neuroscience: realistic modeling for experimentalists*, pages 87–127, 2001.

Tara C. Thiagarajan, Maria Lindskog, and Richard W. Tsien. Adaptation to Synaptic Inactivity in Hippocampal Neurons. *Neuron*, 47(5):725–737, September 2005. doi: 10.1016/j.neuron.2005.06.037. MAG ID: 2031898618 S2ID: dae84bf4b95494656c1fcd90ed1c52be92a0622c.

G. Turrigiano. Homeostatic Synaptic Plasticity: Local and Global Mechanisms for Stabilizing Neuronal Function. *Cold Spring Harbor Perspectives in Biology*, 4(1):a005736–a005736, January 2012. ISSN 1943-0264. doi: 10.1101/cshperspect.a005736. URL http://cshperspectives.cshlp.org/lookup/doi/10.1101/cshperspect.a005736.

Gina G. Turrigiano. The Self-Tuning Neuron: Synaptic Scaling of Excitatory Synapses. *Cell*, 135(3):422–435, October 2008. ISSN 00928674. doi: 10.1016/j.cell.2008.10.008. URL https://linkinghub.elsevier.com/retrieve/pii/S0092867408012981.

Gina G Turrigiano and Sacha B Nelson. Hebb and homeostasis in neuronal plasticity. page 7, 2000.

Gina G. Turrigiano and Sacha B. Nelson. Homeostatic plasticity in the developing nervous system. *Nature Reviews Neuroscience*, 5(2):97–107, February 2004. ISSN 1471-003X, 1471-0048. doi: 10.1038/nrn1327. URL http://www.nature.com/articles/nrn1327.

Gina G. Turrigiano, Kenneth R. Leslie, Niraj S. Desai, Lana C. Rutherford, and Sacha B. Nelson. Activity-dependent scaling of quantal amplitude in neocortical neurons. *Nature*, 391(6670):892–896, February 1998. ISSN 1476-4687. doi: 10.1038/36103. URL https://www.nature.com/articles/36103. Number: 6670 Publisher: Nature Publishing Group.

Corette J. Wierenga, Michael F. Walsh, and Gina G. Turrigiano. Temporal regulation of the expression locus of homeostatic plasticity. *Journal of Neurophysiology*, 96(4): 2127–2133, October 2006. doi: 10.1152/jn.00107.2006. MAG ID: 1971402245 S2ID: cf5feb62d71b0fc42de14d47a062330c97f09e5c.

Ada X Yee, Yu-Tien Hsu, and Lu Chen. A metaplasticity view of the interaction between homeostatic and hebbian plasticity. *Philosophical Transactions of the Royal Society B: Biological Sciences*, 372(1715):20160155, 2017.

C. Zhao, E. Dreosti, and L. Lagnado. Homeostatic Synaptic Plasticity through Changes in Presynaptic Calcium Influx. *Journal of Neuroscience*, 31(20):7492–7496, May 2011. ISSN 0270-6474, 1529-2401. doi: 10.1523/JNEUROSCI.6636-10.2011. URL https://www.jneurosci.org/lookup/doi/10.1523/JNEUROSCI.6636-10.2011.